First- and Second-Order Stress Effects on the Superconducting Transitions of Tantalum and Tin

Abstract: The shift of critical field of a single-crystal wire under uniaxial tension is studied for Ta and Sn. For Ta the shift is nonlinear and gives both the first-order critical field-stress coefficient and a particular combination of second-order coefficients. By combining with other data, the three second-order constants are estimated. The smaller first-order coefficient of Sn is found to be considerably smaller than previous estimates. Both Ta and Sn are found to satisfy a similarity condition for the coefficients, but of a less restrictive form than usual. Similarity is used to predict the behavior of jumps in elastic constant moduli at the transition in Ta. The general formal theory of the first- and second-order coefficients is formulated and many special cases are given. The general thermodynamic relations at the transition between jumps in strain and elastic constants and the various coefficients, are derived. It is shown that BCS theory implies similarity.

I. Introduction

The value of studies of the stress effects on superconducting transitions as a tool for studying the superconducting and normal states of superconducting metals has been shown by the large number of recent papers and by a great variety of new results. A good many results have been fairly well confirmed by cross checks between different workers and different methods, and now more delicate features of the effects can be studied including, for example, anisotropy, second-order effects, and the applicability of similarity. The present work¹ aims to demonstrate the value of, and to apply, the uniaxial stress technique first introduced by C. Grenier,² which measures the magnetic transition on single-crystal wires under uniaxial stress. With this technique it becomes possible to explore in detail the anisotropic nature of the stress effects, and to obtain in some cases second-order coefficients as well as first-order coefficients, i.e., the shift of critical field, H_c , quadratic in the stress components, as well as the linear term. An anisotropic stress can be easily applied, since tension produces both shear and hydrostatic stress, whose direction can be varied by studying differently oriented specimens, and quite sizeable magnitudes are simply obtained by using thin specimens, the limitation being the strength of the material. However, the relative simplicity of the measurement is achieved at the expense of more trouble in specimen preparation. Thus in both the cases studied here, some desired orientations were not obtained, and the measurements had to be supplemented by hydrostatic pressure results although, in principle, complete results (on first-order coefficients) are obtainable by this method alone.

Because interpretation of the data requires analysis of a number of anisotropic stress situations, we take this opportunity to develop the phenomenological theory for general stresses. Some special results are given by Fiske³, and still more in the thesis by Grenier², but we have developed the equations more extensively and systematically. In particular, Section 2 introduces definitions and notations for both first- and second-order critical field stress and strain coefficients, and notes the various special forms for special stresses of interest and for cubic and tetragonal symmetry. Appendices 1 and 2 contain additional relevant material on the description of crystal elasticity and the

relations between the stress and the strain coefficients.

We then develop along standard lines, in Section 3, but introducing a general stress, the general thermodynamic relations between jumps of strain and of elastic constants at the transition and the stress coefficients defined in Section 2. The jumps in elastic constant are of particular interest to us because they can be directly measured and provide an independent source of the second-order coefficients. A careful discussion is given of the meaning of similarity, which has been frequently used to discuss the temperature dependence of the various coefficients. The general equations for these temperature dependences, including the second-order coefficients, are derived for both a less restrictive form of similarity, called *simple* similarity, and a more restrictive form, called double similarity. Finally, it is shown that the BCS description of a superconductor effectively implies simple similarity, deviations from it being very small.

The experimental procedures are described in Section 4, with notes on the specimen preparation and on the design of the tension apparatus to give a direct measure of the tension on the specimen without errors due to friction at supports.

Section 5 presents the data obtained on Ta and Sn, and successively discusses implications which require more and more supplementary information and assumptions. In the Ta analysis we lean heavily on the work on Ta of Jennings and Swenson,4 and Hinrichs and Swenson;⁵ various data used are tabulated in Appendix 3. The measurement of meaningful transition curves for Ta has been made possible only recently through the preparation of specially purified material, and many of the older results are of no value for quantitative discussion. Among the results in this Section are: an evaluation of the first-order constant, which agrees well with various hydrostatic measurements; an estimate of the three second-order constants from these data, the hydrostatic work, and certain sound velocity jump measurements; analysis to show the behavior of the first-order constant with temperature follows simple similarity, although showing a large deviation from double similarity; application of similarity to predict the temperature dependence of the elastic constant jumps at the transition. It is noteworthy that the second-order stress effects appear well within the linear elastic region, and that they are basically shear effects, since the hydrostatic second-order effects at these pressures (and larger) are too small for observa-

The work on Sn concerns only first-order coefficients, because plastic flow limits the maximum tension. Among the results are: the great anisotropy of the stress effect is confirmed and shown to be considerably larger than previously thought; consistency arguments among three measurements are given that indicate a difference between hydrostatic measurements on polycrystalline and single-crystal specimens; evidence

is given for deviation of the temperature dependence of the stress coefficients from double similarity in the same direction as for Ta, Pb and In; some questions are raised about inconsistent results on In and the nature of its deviation from double similarity.

2. Formal theory of critical field-stress and strain relations

2.1 Definitions of the first- and second-order coefficients. The phenomenological parameters of interest in the present work, which characterize certain intrinsic properties of superconductors, are defined by power series expansions of the critical field, H_c , as either a function of the stress components, ϵ_i , i=1 to 6 or of the strain components, ϵ_i , i=1 to 6. In the limit of small stress or strain, the situation considered here, the coefficients of the first-order (linear) and second-order (quadratic) terms in these expansions are the quantities of interest. In this section we introduce a general notation, derive various relations that will be useful in later discussion, and note the effects of symmetry.

First regard H_c as a function of stress, and write for the shift in H_c with stress (the argument σ_i will stand for all six stress components),

$$\begin{split} \Delta_{\sigma}H_c &\equiv H_c(T,\sigma_i) - H_c(T,0) \\ &= \sum_{i=1}^6 \beta_i \sigma_i + \frac{1}{2} \sum_{i,j=1}^6 \beta_{ij} \sigma_i \sigma_j + \text{higher terms} \,. \end{split} \tag{2.1}$$

The first-order critical field-stress coefficients, β_i , are given by the derivatives of H_c , evaluated at zero stress, as

$$\beta_i(T) = (\partial H_c(T, \sigma_i)/\partial \sigma_i)_{T, \sigma_i, i \neq i}, \quad i = 1 \text{ to } 6.$$
 (2.2)

In general they are functions of temperature—but not of stress, since they are properties of the unstressed state.

Similarly, the second-order coefficients are given by

$$\beta_{ij} = \partial^2 H_c / \partial \sigma_i \, \partial \sigma_j \,, \quad i, j = 1 \text{ to } 6 \,. \tag{2.3}$$

The analogous development to (2.1) to (2.3) regarding H_c as a function of strain gives

$$\Delta_{\varepsilon} H_{c} \equiv H_{c}(T, \varepsilon_{i}) - H_{c}(T, 0)$$

$$= \sum_{i=1}^{6} \alpha_{i} \varepsilon_{i} + \frac{1}{2} \sum_{i,j=1}^{6} \alpha_{ij} \varepsilon_{i} \varepsilon_{j} + \text{higher terms}. \qquad (2.4)$$

Again, first- and second-order coefficients appear, related to derivatives of H_c in the unstressed state by

$$\alpha_i(T) = (\partial H_c(T, \varepsilon_i)/\partial \varepsilon_i)_{T,\varepsilon_i,j\neq i}, \quad i = 1 \text{ to } 6,$$
 (2.5)

$$\alpha_{ij} = \partial^2 H_c / \partial \epsilon_i \partial \epsilon_j , \quad i, j = 1 \text{ to } 6.$$
 (2.6)

The stresses and strains are linearly related through the elastic constants by

$$\varepsilon_i = \sum_{j=1}^6 S_{ij} \sigma_j \,, \tag{2.7}$$

$$\sigma_j = \sum_{i=1}^6 C_{ji} \varepsilon_i \,. \tag{2.8}$$

By using the elastic relations (2.7), (2.8) between stress and strain, the α_i 's and α_{ij} 's can be expressed linearly in terms of the β_i 's and β_{ij} 's and vice versa. Details of these relations and the simplified forms for the special cases of cubic and tetragonal symmetry are given in Appendix 2.

2.2 Special forms for cubic symmetry

For crystals with full cubic symmetry, the β_i 's and β_{ij} 's simplify considerably and involve only one and three independent components, respectively; they are given directly by the forms for second-and fourthrank tensors with cubic symmetry, which are, in reduced index notation and referred to the cubic axes,⁷

$$\beta_i = (\beta_1, \beta_1, \beta_1, 0, 0, 0)$$
;

$$\beta_{ij} = \begin{pmatrix} \beta_{11} & \beta_{12} & \beta_{12} & 0 & 0 & 0 \\ \beta_{12} & \beta_{11} & \beta_{12} & 0 & 0 & 0 \\ \beta_{12} & \beta_{12} & \beta_{11} & 0 & 0 & 0 \\ 0 & 0 & 0 & \beta_{44} & 0 & 0 \\ 0 & 0 & 0 & 0 & \beta_{44} & 0 \\ 0 & 0 & 0 & 0 & 0 & \beta_{44} \end{pmatrix}. \tag{2.8}$$

Then the linear and quadratic terms of (2.1) can be written in the forms:

$$\begin{split} \Delta_{\sigma}H_{c} &= \beta_{1}(\sigma_{1} + \sigma_{2} + \sigma_{3}) + \frac{1}{2}\beta_{11}(\sigma_{1}^{2} + \sigma_{2}^{2} + \sigma_{3}^{2}) \\ &+ \beta_{12}(\sigma_{2}\sigma_{3} + \sigma_{3}\sigma_{1} + \sigma_{1}\sigma_{2}) \\ &+ \frac{1}{2}\beta_{44}(\sigma_{4}^{2} + \sigma_{5}^{2} + \sigma_{6}^{2}), \end{split} \tag{2.9}$$

$$&= \beta_{1}(\sigma_{1} + \sigma_{2} + \sigma_{3}) + \frac{1}{6}(\beta_{11} + 2\beta_{12}) \\ &\times (\sigma_{1} + \sigma_{2} + \sigma_{3})^{2} \\ &+ \frac{1}{6}(\beta_{11} - \beta_{12})[(\sigma_{2} - \sigma_{3})^{2} \\ &+ (\sigma_{3} - \sigma_{1})^{2} + (\sigma_{1} - \sigma_{2})^{2}] \\ &+ \frac{1}{2}\beta_{44}(\sigma_{4}^{2} + \sigma_{5}^{2} + \sigma_{6}^{2}). \end{split} \tag{2.10}$$

Under a hydrostatic stress, σ , which is given in component form in the Appendix in (A1.6), we have

$$\Delta_{\sigma} H_c = 3\beta_1 \sigma + \frac{3}{2} (\beta_{11} + 2\beta_{12}) \sigma^2 . \tag{2.11}$$

The usual pressure coefficient of H_c is then obtained by defining the hydrostatic pressure of magnitude $p \equiv -\sigma$, so that

$$\left(\frac{\partial H_c}{\partial p}\right)_T = -\left(\frac{\partial H_c}{\partial \sigma}\right)_T = -3\beta_1. \tag{2.12}$$

Under uniaxial stress, σ , applied in the direction having direction cosines l_1 , l_2 , l_3 with respect to the

crystal axes, with components given by (A1.7), we have

$$\Delta_{\sigma}H_{c} = \beta_{1}\sigma + \left[(\beta_{11}/2)(l_{1}^{4} + l_{2}^{4} + l_{3}^{4}) + (\beta_{12} + \beta_{44}/2)(l_{2}^{2}l_{3}^{2} + l_{3}^{2}l_{1}^{2} + l_{1}^{2}l_{2}^{2}) \right]\sigma^{2}, (2.13a)$$

$$= \beta_{1}\sigma + (\beta_{11}/2)\sigma^{2} + (\beta_{12} + \beta_{44}/2 - \beta_{11})$$

$$\times (l_{2}^{2}l_{3}^{2} + l_{3}^{2}l_{1}^{2} + l_{1}^{2}l_{2}^{2})\sigma^{2}. (2.13b)$$

Under shear stress, σ , along l_1 , l_2 , l_3 in a plane perpendicular to m_1 , m_2 , m_3 , with components given by (A1.8), we have

$$\begin{split} \Delta_{\sigma}H_{c} &= \{(2/3)(\beta_{11} - \beta_{12})[(l_{2}m_{2} - l_{3}m_{3})^{2} \\ &+ (l_{3}m_{3} - l_{1}m_{1})^{2} + (l_{1}m_{1} - l_{2}m_{2})^{2}] \\ &+ (\beta_{44}/2)[(l_{2}m_{3} + l_{3}m_{2})^{2} + (l_{3}m_{1} + l_{1}m_{3})^{2} \\ &+ (l_{1}m_{2} + l_{2}m_{1})^{2}]\}\sigma^{2} \,. \end{split} \tag{2.14}$$

We note that the linear stress terms for both hydrostatic and uniaxial stress lead to the single first-order constant β_1 , but that linear effects vanish for all shears in crystals with cubic symmetry. We also note that the quadratic terms of hydrostatic stress yield one combination of the three second-order constants, $\beta_{11} + 2\beta_{12}$, while quadratic terms of uniaxial stress in two (or more) directions yield both β_{11} and $(\beta_{44} + 2\beta_{12})$, and the quadratic terms of shear stress could give $(\beta_{11} - \beta_{12})$ and β_{44} .

2.3 Special forms for tetragonal symmetry

In crystals with the higher tetragonal symmetries, such as white tin and indium, the β_i and β_{ij} tensors have two and six components respectively; the general forms with respect to the principal axes of the crystal, x_3 being along the tetragonal axis, are⁸

$$\beta_i = (\beta_1, \beta_1, \beta_3, 0, 0, 0)$$
;

$$\beta_{ij} = \begin{bmatrix} \beta_{11} & \beta_{12} & \beta_{13} & 0 & 0 & 0 \\ \beta_{12} & \beta_{11} & \beta_{13} & 0 & 0 & 0 \\ \beta_{13} & \beta_{13} & \beta_{33} & 0 & 0 & 0 \\ 0 & 0 & 0 & \beta_{44} & 0 & 0 \\ 0 & 0 & 0 & 0 & \beta_{44} & 0 \\ 0 & 0 & 0 & 0 & 0 & \beta_{66} \end{bmatrix}. \tag{2.15}$$

Then, for general stress, $\Delta_{\sigma}H_{c}$ becomes from (2.1) and (2.15), keeping only first- and second-order terms,

$$\Delta_{\sigma}H_{c} = \beta_{1}(\sigma_{1} + \sigma_{2}) + \beta_{3}\sigma_{3}$$

$$+ (\beta_{11}/2)(\sigma_{1}^{2} + \sigma_{2}^{2}) + (\beta_{33}/2)\sigma_{3}^{2}$$

$$+ \beta_{12}\sigma_{1}\sigma_{2} + \beta_{13}(\sigma_{2}\sigma_{3} + \sigma_{3}\sigma_{1})$$

$$+ (\beta_{44}/2)(\sigma_{4}^{2} + \sigma_{5}^{2}) + (\beta_{66}/2)\sigma_{6}^{2}. \qquad (2.16)$$

We now discuss the effects of special stresses, but only first-order terms will be retained for later application; in general these terms can be written in the form

$$\begin{split} \Delta_{\sigma} H_c &= \big[(2\beta_1 + \beta_3)/3 \big] (\sigma_1 + \sigma_2 + \sigma_3) \\ &+ \big[(\beta_1 - \beta_3)/3 \big] (\sigma_1 + \sigma_2 - 2\sigma_3) \,, \quad \text{(first order)}. \end{split} \tag{2.17}$$

From (2.17) we see that under hydrostatic stress only the first term is finite and gives $-(2\beta_1 + \beta_3)p$. Under uniaxial stress along l_1 , l_2 , l_3 ,

$$\Delta_{\sigma}H_{c} = [(2\beta_{1} + \beta_{3})/3]\sigma + [(\beta_{1} - \beta_{3})(1 - 3l_{3}^{2})/3]\sigma,$$
(2.18a)

=
$$(\beta_1 \sin^2 \theta + \beta_3 \cos^2 \theta)\sigma$$
, (first order), (2.18b)

where $l_3 = \cos \theta$. Finally, under general shear stress, given by (A1.8), only the second term of (2.17) is finite, and gives

$$\Delta_{\sigma}H_{c} = -2\sigma(\beta_{1} - \beta_{3})l_{3}m_{3}, \quad \text{(first order)}. \tag{2.19}$$

We note that $\Delta_{\sigma}H_{c}$ in (2.19) vanishes for shears in the coordinate planes (1 or m along any of the crystal axes) and has its maximum magnitude for $l_{3}=m_{3}=\pm1/\sqrt{2}$, i.e., for shears in planes at 45° to the tetragonal axis which compress (or expand) the tetragonal axis, and expand (or compress) the transverse axes.

3. Thermodynamic relations at the transition

3.1 The free energy of a superconductor under stress in a magnetic field

The formal relations of Section 2 apply to any intrinsic scalar property, such as H_c , which is a function of a symmetrical second-rank tensor field in the material, such as stress. We now obtain the physical relations between the critical field-stress coefficients and discontinuities in strains and elastic constants at the superconducting transition which are consequences of thermodynamics. The procedure is standard, but we give some steps of the derivation to bring out details of the treatment of a general stress.

The differential of internal energy, E, of a specimen of material under a reversible infinitesimal change of strain $d\varepsilon_i$, and of magnetic moment dM, in a uniform external field H_e with possible absorption of heat, is

$$dE = T dS + V \sum_{i=1}^{6} \sigma_i d\varepsilon_i + H_e dM, \qquad (3.1)$$

where we assume homogeneous strain throughout the volume V; S is the entropy.

Define a Gibbs free energy for the specimen by

$$G(T, \sigma_i, H_e) \equiv E - TS - V \sum_{i=1}^{6} \sigma_i \varepsilon_i - H_e M ; \qquad (3.2)$$

hence, from (3.1),

$$dG = -S dT - V \sum_{i=1}^{6} \varepsilon_i d\sigma_i - M dH_e.$$
 (3.3)

In (3.3) we neglect second-order strain terms like $\sigma_i \varepsilon_i dV$, and treat ε_i as infinitesimal at all times.

At the phase transition, considered to take place reversibly at constant T, σ_i and $H_e(=H_c)$, the change in G in going from the superconducting to the normal state is, from (3.3),

$$\Delta_{tr}G \equiv G_{r}(T,\sigma_{i}) - G_{s}(T,\sigma_{i},H_{c}) = 0, \qquad (3.4)$$

where we indicate by omission of the argument H_c that the free energy of the normal state, $G_n(T, \sigma_i)$, is independent of magnetic field (we ignore the weak susceptibility of a normal metal). Equation (3.4) implicitly defines the critical field as a function of T and σ_i , $H_c(T, \sigma_i)$.

Also from (3.3) the change of G_s in a field H_e is

 $G_s(T, \sigma_i, H_e)$

$$= G_s(T, \sigma_i, 0) - \int_0^{H_e} M \ dH_e \ , \tag{3.5a}$$

$$= G_s(T, \sigma_i, 0) + \int_0^{H_e} V_s(T, \sigma_i, H_e) H_e dH_e / 4\pi , \quad (3.5b)$$

where the relation for a perfect diamagnet,

$$M = -V_s H_e / 4\pi , \qquad (3.6)$$

has been used for the magnetic moment of the superconductor of volume V_s in a uniform field H_e , thus ignoring penetration effects—a good approximation for superconductors of macroscopic dimensions.

3.2 Relations at the transition; magnetostrictive and transition changes of strain

The quantity V_s has been retained under the integral sign in (3.5b) to indicate a dependence on H_e , namely, the magnetostrictive effect of the external field on the superconductor. In fact, this dependence is a higher order strain effect which could be neglected, but is convenient to retain at this point. We can evaluate the magnetostrictive strain by differentiating (3.5b) with respect to σ_i , and using (3.3), to give,

$$V_s[\varepsilon_i(T, \sigma_i, H_e) - \varepsilon_i(T, \sigma_i, 0)]$$

$$= -\int_{0}^{H_e} \left(\frac{\partial V_s}{\partial \sigma_i}\right)_{T,H_e,\sigma_i,j\neq i} H_e dH_e/4\pi , \qquad (3.7)$$

where the higher order term coming from the change of V_s with H_e has been neglected on the left.

By inserting (3.5b) with $H_e = H_c$ into (3.4), we obtain the well-known equation for the difference in intrinsic free energies of normal and superconducting states in zero field, namely,

$$G_n(T, \sigma_i) - G_s(T, \sigma_i, 0)$$

$$= \int_{0}^{H_{c}(T,\sigma_{i})} V_{s}(T,\sigma_{i},H_{e})H_{e} dH_{e}/4\pi . \qquad (3.8)$$

Differentiation of (3.8) with respect to σ_i gives

$$V[\varepsilon_{i}^{n}(T,\sigma_{i}) - \varepsilon_{i}^{s}(T,\sigma_{i},0)]$$

$$= -V_{s}(T,\sigma_{i},H_{c})(H_{c}/4\pi)(\partial H_{c}/\partial \sigma_{i})$$

$$-\int_{0}^{H_{c}} (\partial V_{s}/\partial \sigma_{i})H_{e} dH_{e}/4\pi , \qquad (3.9)$$

where on the left, the difference between V_s and V_n has been neglected. Comparison of (3.9) and (3.7) shows that the difference in strain ε_i , for given stress σ_i , between the normal and superconducting states in zero field, may be considered made up of two parts—a magnetostrictive part, which builds up continuously with field as H_e increases to H_c , and a transition part which occurs discontinuously during the transition at H_c . The latter part we may write, using (2.2),

$$\Delta_{tr} \varepsilon_{i} \equiv \varepsilon_{i}^{n}(T, \sigma_{i}) - \varepsilon_{i}^{s}(T, \sigma_{i}, H_{c})$$

$$= -\frac{H_{c}}{4\pi} \frac{\partial H_{c}}{\partial \sigma_{i}} \equiv -\frac{H_{c}\beta_{i}}{4\pi}.$$
(3.10)

We note that the magnetostrictive change in strain, (3.7), can be written

$$\Delta_{H_e} \varepsilon_i^s \equiv \varepsilon_i^s (T, \sigma_i, H_e) - \varepsilon_i^s (T, \sigma_i, 0)$$

= $-(S_{1i} + S_{2i} + S_{3i}) H_e^2 / 8\pi$, (3.11)

on neglecting the change of $(\partial V_s/\partial \sigma_i)$ with H_e , and using (A1.4a).

From (3.10) by differentiating with respect to T, the jump in components of the tensor of thermal expansion coefficients, $\partial \varepsilon_i/\partial T$, i=1 to 6, at the transition is immediately expressed in terms of H_c , $\partial H_c/\partial T$, β_i , $\partial \beta_i/\partial T$. Also note that, from (3.10), (2.1) and (A1.6)

$$\begin{split} \Delta_{\rm tr} V &= V(\Delta_{\rm tr} \varepsilon_1 + \Delta_{\rm tr} \varepsilon_2 + \Delta_{\rm tr} \varepsilon_3) \\ &= -\frac{V H_c}{4\pi} (\beta_1 + \beta_2 + \beta_3) = \frac{V H_c}{4\pi} \frac{\partial H_c}{\partial n} \,, \end{split}$$

the usual formula for the simple hydrostatic case.

3.3 Change of elastic modulus at the transition

A direct consequence of Eq. (3.10) for the jump in strain at the transition, is the jump in elastic constants at the transition, obtained by differentiating again with respect to σ_j ; this gives, using (A1.4a) or $(\partial \varepsilon_i/\partial \sigma_j) = S_{ij}$,

$$\Delta_{tr}S_{ij} = -\frac{1}{4\pi} \left[\frac{\partial H_c}{\partial \sigma_i} \frac{\partial H_c}{\partial \sigma_j} + H_c \frac{\partial^2 H_c}{\partial \sigma_i \partial \sigma_j} \right],$$

$$= -(\beta_i \beta_i + H_c \beta_{ii})/4\pi . \quad \text{(Footnote 10)}. \quad (3.12)$$

Thus the jumps in elastic compliance coefficients are linearly related to the second-order stress coefficients of H_c . We note that $\Delta_{\rm tr}S_{ij}$ is finite in general at $T=T_c$, where $H_c=0$, as expected when the transition is second order, whereas $\Delta_{\rm tr}\varepsilon_i$ vanishes there.

For cubic symmetry, (3.12) reduces to the three relations

$$\Delta_{tr} S_{11} = \Delta_{tr} S_{22} = \Delta_{tr} S_{33}$$

$$= -(\beta_1^2 + H_c \beta_{11})/4\pi , \qquad (3.13a)$$

$$\Delta_{\rm tr}S_{12}=\Delta_{\rm tr}S_{13}=\Delta_{\rm tr}S_{23}$$

$$= -(\beta_1^2 + H_c \beta_{12})/4\pi , \qquad (3.13b)$$

$$\Delta_{\rm tr} S_{44} = \Delta_{\rm tr} S_{55} = \Delta_{\rm tr} S_{66} = -H_c \beta_{44}/4\pi$$
 (3.13c)

At T_c , $\Delta_{\rm tr}S_{44}=0$, corresponding to the vanishing of linear shear effects for cubic symmetry. We can, in fact, find direct relations between the shift in H_c under special stresses, such as uniaxial and hydrostatic stress, and the corresponding elastic constants. Thus, the jump in the reciprocal Young's modulus, $\Delta_{\rm tr}(1/Y)$, given as a function of direction by (A1.13) is very simply related by (3.13) to the shift of H_c under uniaxial stress given by (2.13b), namely,

$$\begin{split} \Delta_{\sigma}H_{c} &= \beta_{1}\sigma - \frac{{\beta_{1}}^{2}\sigma^{2}}{2H_{c}} \\ &- \frac{4\pi\sigma^{2}}{2H_{c}} \, \Delta_{\rm tr}\!\left(\!\frac{1}{Y}\!\right) \,, \quad \text{(uniaxial stress)}. \end{split} \tag{3.14}$$

Similarly, from (A1.12), (A1.10b), and (2.11), the jump in reciprocal bulk modulus (1/B) at the transition is related to the shift of H_c under hydrostatic stress by

$$\begin{split} \Delta_{\sigma}H_{c} &= 3\beta_{1}\sigma - \frac{3{\beta_{1}}^{2}\sigma^{2}}{H_{c}} \\ &- \frac{2\pi\sigma^{2}}{H}\,\Delta_{\mathrm{tr}}\!\left(\!\frac{1}{B}\!\right), \quad \text{(hydrostatic stress)}. \quad (3.15) \end{split}$$

It is also useful to express directly the jump at H_c in the special elastic moduli corresponding to particular, directly observed, sound velocities in terms of the β_{ij} and β_1 , using (A1.10) to relate the S_{ij} and C_{ij} , and (A1.11) to define the elastic moduli. This gives

$$\Delta_{\rm tr} C = (H_c/4\pi)C^2\beta_{44} \,, \tag{3.16a}$$

$$\Delta_{tr}C' = (H_c/2\pi)C'^2(\beta_{11} - \beta_{12}), \qquad (3.16b)$$

$$\Delta_{\text{tr}}C_L = 9B^2\beta_1^2/4\pi + (H_c/4\pi)[3B^2(\beta_{11} + 2\beta_{12}) + C^2\beta_{44} + (2C'^2/3)(\beta_{11} - \beta_{12})], \qquad (3.16c)$$

where, from (A1.12),

$$B = C_L - C - C'/3. (3.17)$$

Thus, measurements of the three velocity jumps and velocities, with knowledge of β_1 and H_c , will determine the three second-order coefficients β_{11} , β_{12} , β_{44} .

3.4 Similarity and the temperature dependence of stress coefficients

A useful description of the behavior of the critical field-temperature relation under stress is given by assumption of the so-called similarity conditions. These assumptions permit the temperature dependence of β_i and β_{ij} to be calculated from their values at either one or two temperatures plus knowledge of the critical field curve at zero stress. Similarity, although not exact, seems to be a good approximation in many cases, and in general it is helpful to describe behavior in terms of deviations from similarity. Accordingly, we now develop explicit formulas for the calculation of $\beta_i(T)$ and $\beta_{ij}(T)$ which will be used later in analysis of various measurements. We take this occasion to state carefully the two separate similarity conditions, to develop their implications separately, and to generalize the entire analysis to the case of general stress, in place of the usual hydrostatic pressure.

The first similarity condition states that the entire family of critical field curves under stress can be described in terms of a single function f(x) whose functional form is independent of stress, by

$$\frac{H_c(T,\sigma_i)}{H_0(\sigma_i)} = f\left(\frac{T}{T_c(\sigma_i)}\right),\tag{3.18}$$

where

$$f(0) \equiv 1$$
, $f(1) \equiv 0$.

Thus at any stress σ_i , i=1 to 6, the same reduced critical field curve applies, where two parameters are used to reduce H_c and T, namely $H_0(\sigma_i)$, the critical field at 0° K, and $T_c(\sigma_i)$, the critical temperature. Note that f can be different for different superconductors, so the assumption (3.18) is less restrictive than is assuming a universal reduced equation of state for all superconductors.

Further simplification of the description is obtained by assuming that a second similarity condition is also obeyed, namely,

$$\frac{H_0(\sigma_i)}{T_c(\sigma_i)} = \frac{H_0(0)}{T_c(0)} \,. \tag{3.19}$$

Thus the two parameters of the reduced equation are reduced to one.

The significance of (3.19) is indicated by the Kok relation for the electronic heat capacity coefficient of the normal state, 11 γ ,

$$\gamma = -\frac{VH_0}{4\pi} \left(\frac{\partial^2 H_c}{\partial T^2}\right)_{T=0}.$$
 (3.20a)

Equation (3.20a) is simply a consequence of thermodynamics (and the assumption that the superconducting specific heat has no term linear in T). Now if the first similarity condition (3.18) holds, then (3.20a) takes the form

$$\gamma = -\frac{V}{4\pi} f''(0) \left(\frac{H_0}{T_c}\right)^2, \tag{3.20b}$$

where f''(0) is a constant fixed by the functional form of f(x). Now for change of isotopic mass, the original

case in which similarity was applied, γ , being a property of the electronic distribution, is expected to change very little. Hence, in this case, from (3.20b), the first similarity condition leads to the second.

Stress, however, would in general be expected to alter the electron distribution and γ , (and also V) hence, from (3.20b), also H_0/T_c ; the deviation from (3.19) would then be related to the variation of γ with stress. Since, in fact, (3.18) is more commonly satisfied than (3.19), we shall derive results both on the basis of (3.18) above (simple similarity) and for (3.18) and (3.19) (double similarity).

For convenience in manipulation we introduce a compact notation, and write

$$H_c = H_0 f(t), \quad t = T/T_c.$$
 (3.21)

Now, by differentiating with respect to σ_i or T, we obtain relations for various critical field-stress or temperature coefficients. We have

$$H_{c,T} \equiv \partial H_c / \partial T = H_0 f' / T_c , \qquad (3.22)$$

where f' is the derivative with respect to the single argument of f, and

$$H_{c,i} \equiv \partial H_c / \partial \sigma_i = H_{0,i} (f - f' t \delta_i) , \qquad (3.23)$$

where

$$\delta_i \equiv (H_0 T_{c,i} / T_c H_{0,i})$$

$$= (\partial \ln T_c / \partial \sigma_i) / (\partial \ln H_0 / \partial \sigma_i) , \qquad (3.24)$$

$$H_{0,i} = \partial H_0 / \partial \sigma_i \,, \tag{3.25}$$

$$T_{c,i} = \partial T_c / \partial \sigma_i$$
 (Ref. 12). (3.26)

A second differentiation gives either

$$H_{c,TT} = H_0 f''/T_c^2, (3.27)$$

or

$$H_{c,iT} \equiv (\partial^2 H_c/\partial \sigma_i \partial T)$$

= $(H_{0,i}/T_c)[f'(1-\delta_i)-f''t\delta_i],$ (3.28a)

$$\begin{split} H_{c,ij} &\equiv (\partial^2 H_c/\partial \sigma_i \partial \sigma_j) = H_{0,ij} (f - \delta_{ij}) \\ &+ (H_{0,i} H_{0,j} / H_0) t \big[f'(2\delta_i \delta_j - \delta_i - \delta_j) + f'' t \big] \,; \\ \delta_{ij} &= H_0 T_{c,ij} / T_c H_{0,ij} \,, \end{split} \tag{3.28b}$$

and a third differentiation leads finally to

$$H_{c,ijT} \equiv (\partial^{3} H_{c}/\partial \sigma_{i} \partial \sigma_{j} \partial T) = (1/T_{c}) \{ H_{0,ij} f' - (H_{0} T_{c,ij}/T_{c}) (f' + f''t) + (H_{0,i} H_{0,j}/H_{0}) [(2\delta_{i}\delta_{j} - \delta_{i} - \delta_{j}) (f' + tf'') + t(2f'' + tf''')] \}.$$
(3.29)

Equations (3.21) to (3.29) are based only on simple similarity. Assuming $H_0(0)$, $T_c(0)$, f(t) are known functions, then $\beta_i(T) \equiv H_{c,i}(T, 0)$ is determined by

(3.23) when the two constants $H_{0,i}(0)$ and $\delta_i(0)$ are known. If β_i is measured at two temperatures, or if $\beta_i(T)$ and $d\beta_i/dT \equiv H_{c,iT}$ (given by (3.28a)) are known at some T, such as T_c , then $H_{0,i}(0)$ and $\delta_i(0)$ can be found.

Similarly for the second-order coefficients, if $H_0(0)$, $T_c(0)$, f(t), $\beta_i(T)$, $\beta_j(T)$, $\delta_i(0)$, $\delta_j(0)$ are known, then $\beta_{ij}(T) = H_{c,ij}$ is determined by (3.28b) if the two constants $H_{0,ij}$ and $T_{c,ij}$ are known. Again measurements of β_{ij} at two temperatures or of β_{ij} and $d\beta_{ij}/dT = H_{c,ijT}$ (given by (3.29)) will determine the two constants.

If the second similarity condition is also true, then the two constants in each case are related, since

$$\frac{H_{0,i}(\sigma_i)}{T_{c,i}(\sigma_i)} = \frac{H_{0i,j}(\sigma_i)}{T_{c,i,j}(\sigma_i)} = \frac{H_0(0)}{T_c(0)}, \quad \delta_i = \delta_j = 1, \quad (3.30)$$

and (3.23) to (3.29) become

$$H_{c,i} = H_{0,i}(f - f't)$$
, (3.31)

$$H_{c,T} = -(H_{0,i}/T_c)f''t, (3.32)$$

$$H_{c,ij} = H_{0,ij}(f - f't) + (H_{0,i}H_{0,i}/H_0)t^2f'',$$
 (3.33)

$$H_{c,i,i,T} = (1/T_c) [-H_{0,i,i}f''t]$$

+
$$(H_{0,i}H_{0,j}/H_0)t(2f'' + tf''')$$
]. (3.34)

Now only a single value of β_i , or β_{ij} , is required to fix the T dependence everywhere.

If we have both cubic symmetry and double similarity, the explicit formulas for the β 's are simply

$$\beta_1(T) = H_{0,1}(f - f't),$$
 (3.35a)

$$\beta_{11}(T) = H_{0.11}(f - f't) + (H_{0.1}^2/H_0)t^2f'', \qquad (3.35b)$$

$$\beta_{12}(T) = H_{0.12}(f - f't) + (H_{0.1}^2/H_0)t^2f'',$$
 (3.35c)

$$\beta_{44}(T) = H_{0.44}(f - f't). \tag{3.35d}$$

Finally we note that $T_{c,i}$, $T_{c,ij}$ may be evaluated from measurements of H_c , $H_{c,i}$, $H_{c,iT}$, $H_{c,ij}$ near T_c , which is useful in the application of (3.23), (3.28b) in the case of simple similarity. The relations follow from implicit differentiation of the functional relation defining $T_c(\sigma_i)$, namely

$$H_c(T, \sigma_i) = 0, (3.36)$$

which yields

$$T_{c,i} = -H_{c,i}/H_{c,T_c}, (3.37)$$

$$T_{c,ij} = [H_{c,T_c}(H_{c,i}H_{c,jT_c} + H_{c,j}H_{c,iT_c}) - H_{c,T_c}^2 H_{c,ij} - H_{c,i}H_{c,j}H_{c,T_cT_c}]/H_{c,T_c}^3, (3.38)$$

where

$$H_{c,T_c} \equiv (\partial H_c(T, \sigma_i)/\partial T)_{T=T_c}$$

3.5 Similarity and the BCS theory of superconductivity
Although the model of a superconductor developed
by Bardeen, Cooper and Schrieffer¹³ is a simplified

one, which omits many features of a real metal, it has been notably successful in describing quantitatively the behavior of reduced properties of superconductors, i.e., properties scaled with respect to values or parameters fixed by experiment. Similarity is just such a property, hence it is noteworthy that BCS theory effectively predicts simple similarity under stress; however, the second similarity condition will not hold. Actually, the theory provides a mechanism for altering the reduced critical field curve, $H_c(T)/H_0$, under stress, but it turns out that the dependence on stress (through that mechanism) is so weak that similarity is predicted to hold to a high degree of precision and certainly within the experimental accuracy.

To draw this conclusion, we transform the equations of the theory by elimination and combination of parameters to give

$$H_c(T)/H_0 = F(T/T_c, kT_c/\hbar\omega), \qquad (3.39)$$

where F(x, y) is an explicitly known function of its two variables. In particular, the coupling energy V, whose magnitude and stress dependence are not known directly from measurement, has been eliminated and the ratio of kT_c to the phonon energy, $\hbar\omega$, introduced as a dimensionless measure of the electron-phonon coupling strength. The values and stress dependence, or at least pressure dependence, of kT_c and $\hbar\omega = k\Theta$, where Θ is essentially the Debye temperature, can be obtained from measurements independently of the theory. Under stress T_c , Θ and T_c/Θ will in general alter, hence the form of $H_c(T)/H_0$ as a function of T/T_c will change, and similarity will not strictly hold, but a quantitative estimate shows the change to be negligible.

We estimate from the theory that the maximum value of $\partial F/\partial(kT_c/\hbar\omega)$, as a function of T, is about 0.01 for, say, Ta or Sn, for which $(kT_c/\hbar\omega) \cong 0.02$ (Footnote 14).

For estimates of the change of coupling parameter under stress, we use measured values of the effects of pressure on T_c and Θ . Thus we have

$$\frac{\partial \ln(kT_c/\hbar\omega)}{\partial p} = \frac{\partial \ln T_c}{\partial p} - \frac{\partial \ln \Theta}{\partial p} \sim -10^{-6} \text{ atm}^{-1} \text{ for Ta},$$
$$-10^{-5} \text{ atm}^{-1} \text{ for Sn.} \quad \text{(Footnote 15)}$$

Finally, we estimate the variation of F with pressure as

$$\frac{\partial F}{\partial p} = \frac{\partial F}{\partial (kT_c/\hbar\omega)} \frac{kT_c}{\hbar\omega} \frac{\partial \ln(kT_c/\hbar\omega)}{\partial p}$$

$$\sim 0.01 \times 0.02 \times \begin{cases} 10^{-6} \text{(Ta)} \\ 10^{-5} \text{(Sp)} \end{cases} \tag{3.40}$$

 $\sim 10^{-10}/\text{atm}$ for Ta and $10^{-9}/\text{atm}$ for Sn, which is small compared to, say, $\partial \ln T_c/\partial p \sim 10^{-6}$ and $10^{-5}/\text{atm}$, respectively. Thus, effectively, the first similarity condition holds, although, of course, the second

similarity condition will not hold, in general, by the same argument given in Section 3.4, based on Eq. (3.20).

In fact, BCS theory predicts more than desired, since it gives a very close family of functions for the reduced curve $H_c(T)/H_0$, over the possible variation with coupling parameter. Thus, the variation of coupling parameter $kT_c/\hbar\omega$ from zero up to a maximum of about 0.075, the value for Pb, produces only about a 0.3% maximum change in $H_c(T)/H_0$, whereas the observed maximum variation of $H_c(T)/H_0$ in going from A1 to Pb is about 7%. Although the $H_c(T)/H_0$ curves of the theory thus show less sensitivity to the variation of coupling strength among superconductors than is observed, the sensitivity to pressure seems of still smaller magnitude, since the coupling strength itself is a weak function of pressure, and this feature might plausibly persist when the theory is adequately modified to explain the differences among superconductors.

4. Experimental technique

4.1 Preparation of single-crystal specimens

The tin crystals were grown by the following technique. The 99.999% tin metal was heated in a glass vacuum chamber and then forced by helium gas into evacuated 0.043 in. i.d. glass tubes (ten at a time). A furnace with a gradient in temperature was positioned so that decreasing the current to the furnace allowed the tin to solidify progressively down the tubes toward the molten reservoir. The glass tubes were then dissolved in HF. The crystals were subsequently placed in fresh glass tubes for annealing overnight at 190°C in vacuum.

The preparation of the tantalum crystals has been described in an earlier report. In general, they were 2 to 3 inches long and 0.010 in. diameter. The resistivity ratios were purposely controlled to be of the order of $R_{300}/R_{4.2} \sim 300$. In this case the crystals are reasonably strong and have fairly sharp transitions.

4.2 Apparatus for applying uniaxial stresses

The apparatus for applying uniaxial stresses is shown in simplified form in Fig. 1. The essential parts are: a micrometer head, a double-spring balance, and a dial gauge which can be read to 0.0001 inch. Rotation of the micrometer head moves the top of the double spring 0.0249 inch per revolution in calibrated steps, while the dial gauge measures the deflection of the bottom of the spring. The difference between the two extensions is the spring extension, which is proportional, through a calibrated constant, to the stress in the spring. The bottom of the spring is connected through a shaft to one end of the crystal while the other end of the crystal is fixed. Thus the tension in the spring is equal to that in the specimen. There are no frictional constraints in this apparatus to complicate calculation of the stress; the present apparatus differs from Grenier's in this respect.

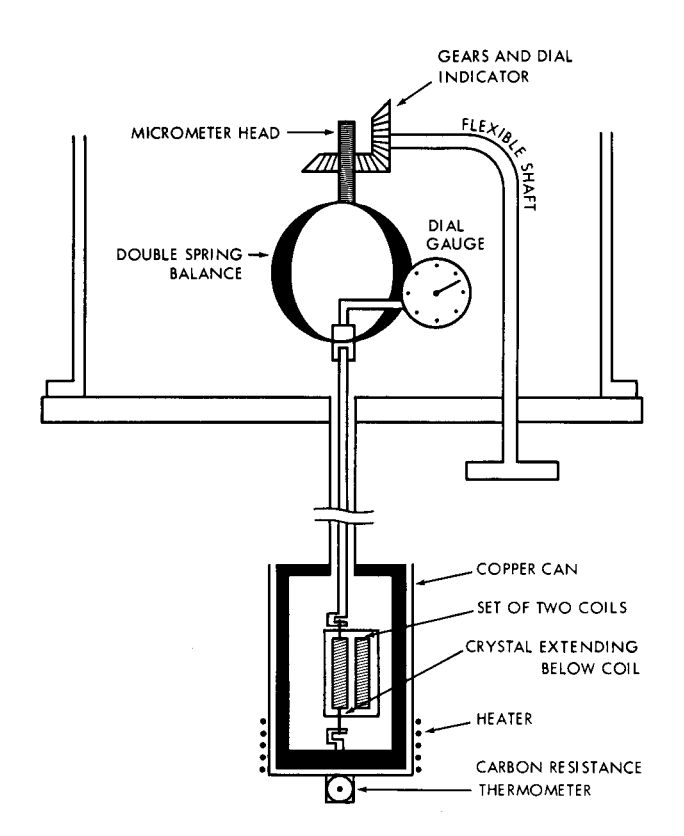


Figure 1 The apparatus for applying uniaxial stresses showing friction-free nature of the determination of stress on the specimen.

The ends of the crystals are gripped by short copper cylinders, into which they are soldered in the case of tin (using nonsuperconducting solder). They are gripped by spot welding to molybdenum rings in the case of tantalum. These grips are hooked onto the apparatus. This method of mounting the specimen leaves it partly free to twist or bend with tension, but it is probably restricted by the copper grips in shearing motion. For tantalum crystals of any orientation and for tin crystals with cylinder axis $\langle 100 \rangle$, $\langle 010 \rangle$, or $\langle 001 \rangle$ this constraint is of no significance. For other orientations of tetragonal crystals, there will be an appropriate correction to allow for the additional constraint.

The diameters of the crystals were chosen so that the stress at the yield point of the metal may be measured with an accuracy on the order of 0.5%. This is also the accuracy with which the average diameter of the specimens is determined.

A bell jar resting on the top plate encloses the apparatus. The micrometer head is rotated through a gear and flexible shaft coupled to a solid shaft entering the top plate through an O-ring seal.

4.3 Pressure and temperature control

Rough control of the pressure above the helium bath is achieved with a Wallace and Tiernan manostat.

A Sommers type bridge circuit¹⁷ and amplifier, working off a carbon resistor, feeds back current to a wire heater (noninductively wound) on the copper can enclosing the specimens. The temperature can be held constant to better than 4×10^{-5} °K throughout two consecutive sets of measurements making up susceptibility curves for the stressed and unstressed crystals. The time required for two sets may be only 10 minutes if the susceptibility curve is sharp.

4.4 Measurement of magnetic moment

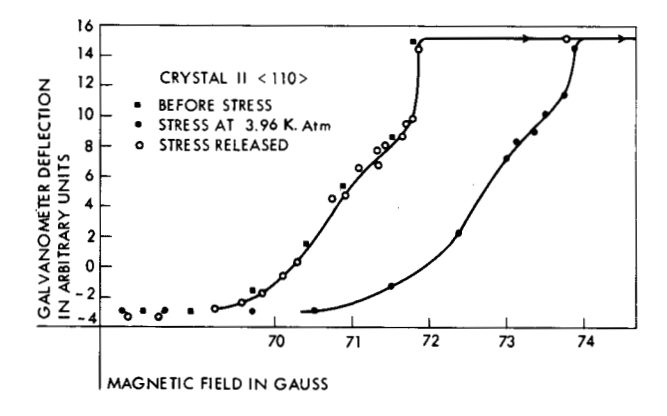
A null technique is used for measuring the magnetic moment of the specimen. Two coils of nearly equal inductance are connected in opposition through the high-sensitivity galvanometer. One coil encloses the center portion of a crystal (the demagnetizing factor for the long, thin cylindrical crystals is essentially eliminated by this technique), while the other coil stands close to the first and parallel to it. The deflection of the galvanometer is measured as a function of the current switched off in a Garret¹⁸ coil. The Garret coil (calibrated by proton resonance) is a large one which surrounds the outer nitrogen dewar. The horizontal component of the earth's field is compensated for by a Helmholtz pair.

5. Observed data and calculated results

5.1 Uniaxial stress data for Ta

A typical set of magnetic moment measurements as a function of applied field on a tantalum specimen are shown in Fig. 2. The effect of the stress is essentially to translate the curve; $\Delta_{\sigma}H_{c}$ was taken from an average value of the translation of the central portion of the curve. The reversibility of the application of the stress is shown by close restoration of the original curve on release of stress; reversibility was checked in this way for most values of stress. The critical field shifts $\Delta_{\sigma}H_{c}$ obtained in measurements on two specimens

Figure 2 Magnetic moment vs applied magnetic field for tantalum crystal #2, axis orientation (110). Points before applying stress, #; points at uniaxial stress of 3.96 k. atm, •; points after stress is released, O.



with the same crystal orientation, axis along $\langle 110 \rangle^{19}$, up to uniaxial stresses σ of nearly 6,000 atm are shown in Fig. 3, which plots $\Delta_{\sigma}H_c/\sigma$ vs σ . The data closely fit an inclined straight line, indicating both a linear and a quadratic stress effect, and the line drawn is obtained by least squares fit to the data, weighted by estimates of uncertainty due to temperature drift, and precision of the galvanometer readings.

From (2.13) with σ applied along $\langle 110 \rangle$, we have

$$\Delta_{\sigma}H_{c} = \beta_{1}\sigma + \frac{1}{4}(\beta_{11} + \beta_{12} + \beta_{44}/2)\sigma^{2}$$
, (\langle 110 \rangle). (5.1)

Hence the least squares line yields

$$\beta_1 = (2.89 \pm 0.13) \times 10^{-4} \text{ gauss/atm},$$
 (5.2a)

$$\frac{1}{4}(\beta_{11} + \beta_{12} + \beta_{44}/2)$$

$$=(3.11 \pm 0.40) \times 10^{-8} \text{ gauss/atm}^2$$
, (5.2b)

all values applying at T_c .

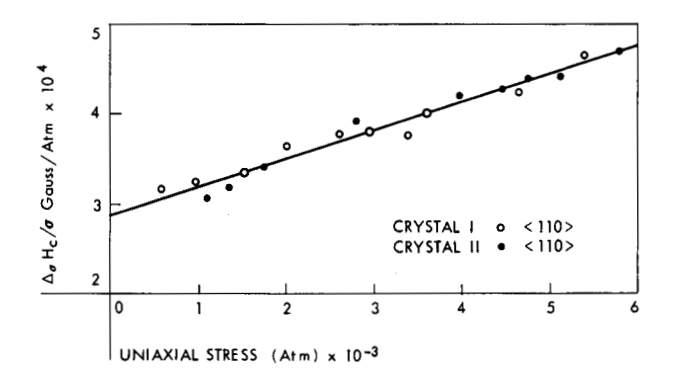
From (5.2a) and (2.12) we obtain for Ta

$$\left(\frac{\partial H_c}{\partial p}\right)_{T_c} = -(8.67 \pm 0.39) \times 10^{-4} \text{ gauss/atm}, \quad (5.3)$$

which may be compared with the value -9.26×10^{-4} gauss/atm of Hinrichs and Swenson,⁵ and the value -8.76×10^{-4} gauss/atm obtained from dT_c/dp of Jennings and Swenson⁴ and critical field data, as described in Section 5.2. Many of the older measurements, using less pure Ta, gave values of $(\partial H_c/\partial p)_{Tc}$ several times these values,²⁰ but the agreement established by Hinrichs and Swenson,⁵ and by the uniaxial stress measurements above, all using specially purified Ta, seems fairly conclusive.

5.2 Calculated results for Ta using critical field data The value of dT_c/dp , or $dT_c/d\sigma_1$, may be obtained

Figure 3 Critical field shift, Δ_σH_c, divided by uniaxial stress, σ, vs σ, for two single-crystal specimens of tantalum, both with (110) orientation. Crystal #1, ο; crystal #2, •; straight line is weighted least squares fit, temperature about 4.27°K.



from $(\partial H_c/\partial p)_{Tc}$ or β_1 by using (3.37), and (A3.4a) for $(\partial H_c/\partial T)_{Tc}$ to give

$$\frac{dT_c}{dp} = -3 \frac{dT_c}{d\sigma_1} = -(2.57 \pm 0.13) \times 10^{-6} \text{ deg/atm.}$$
(5.4)

This may be compared with the measured value of Jennings and Swenson⁴ of $-(2.6 \pm 0.1) \times 10^{-6}$ deg/atm.

The three second-order coefficients β_{11} , β_{12} , β_{44} may now be estimated at T_c by combining information from three sources. These are (1) the uniaxial stress result in (5.2b), (2) the hydrostatic pressure measurement⁴ and (3) the elastic constant discontinuity at the transition curve.²¹ Source (2) gives no significant second-order pressure effect on T_c out to 10,000 atm, or, more precisely, leads to $d^2T_c/dp^2 < 10^{-11}$ deg/atm², on allowing for a possible second-order effect buried in the scatter. Then relating $(\partial^2 H_c/\partial p^2)_{Tc}$ to d^2T_c/dp^2 by (3.38), we have, using (2.11),

$$\beta_{11} + 2\beta_{12} = \frac{1}{3}(\partial^2 H_c/\partial p^2)$$

$$< 10^{-9} \text{ gauss/atm}^2$$
 (Footnote 22) (5.5)

which is negligible compared to the magnitude of the β_{ij} of 10^{-7} given by (5.2b). Source (3) (of data on the second order coefficients β_{ij}) makes use of (3.16), in particular (3.16a), applied to measured values of the jump in the modulus $C=C_{44}$ along the transition curve. To obtain a value at T_c requires extrapolation, since ΔC vanishes at T_c ; hence, using values of H_c from (A3.3), measured values of $\Delta C/C$ ranging from 7.8×10^{-6} at 1.5° K to 1.1×10^{-6} at 4.0° K, with $T_c=4.25^{\circ}$ K, we estimate tentatively by extrapolation that at T_c

$$\beta_{44} \cong 1.6 \times 10^{-7} \text{ gauss/atm}^2$$
, (5.6)

while at lower temperatures it rises to a maximum of about 2.0×10^{-7} at t = 0.65, then falls to 1.6×10^{-7} at t = 0.2. Combining (5.2b), (5.5) and (5.6) yields at T

$$\beta_{11} = 0.8 \times 10^{-7} \text{ gauss/atm}^2,$$
 (5.7a)

$$\beta_{12} = -0.4 \times 10^{-7} \text{ gauss/atm}^2,$$
 (5.7b)

$$\beta_{44} = 1.7 \times 10^{-7} \text{ gauss/atm}^2$$
 (5.7c)

5.3 Calculated results for Ta using critical field data and similarity

We now show that it is possible to deduce the temperature dependence of β_1 up to T_c from $H_c(T)$ using similarity, and fitting one additional parameter. The general equation is (3.23), which we rewrite for the one linear coefficient of the cubic case,

$$\beta_1(T) = (dH_0/d\sigma_1)(f - \delta_1 f't)$$
 (5.8a)

$$\delta_1 \equiv H_0(dT_c/d\sigma_1)/(T_c dH_0/d\sigma_1) . \tag{5.8b}$$

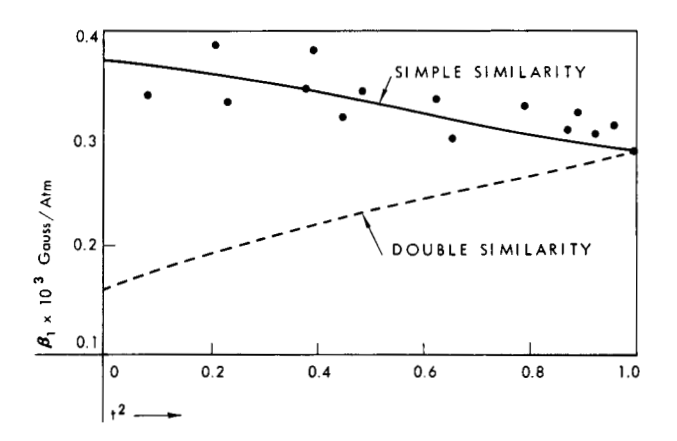


Figure 4 Predicted curve of $\beta_1(t)$ for Ta (solid curve) vs t^2 using simple similarity, critical field data, $\beta_1(T_c)$ and choosing the value of $dH_0/d\sigma_1$ for best fit, Eq. $\beta_1=3.7\times 10^{-4}$ (f=0.43f't) gauss/atm. Points are measured values of Hinrichs and Swenson.⁵ Dashed curve shows prediction of double similarity, Eq. $\beta_1=1.58\times 10^{-4}$ (f=f't) gauss/atm.

In general (5.8a) may be fitted at two values of $\beta_1(T)$ to fix $dH_0/d\sigma_1$ and δ_1 —one of these, however, may be the value at T_c , which we already know. We have from (3.37) and (3.22) at T_c ,

$$\frac{dT_c}{d\sigma_1} = -T_c \beta_1(T_c) / H_0 f'(1) , \qquad (5.9)$$

hence putting (5.9) in (5.8b)

$$\delta_1 = -\beta_1(T_c)/(dH_0/d\sigma_1)f'(1). \tag{5.10}$$

For Ta, then, using (5.2a) for $\beta_1(T_c)$, (A3.4a) for f'(1), (5.10) gives

$$\delta_1 = 1.58 \times 10^{-4} / (dH_0 / d\sigma_1) \,. \tag{5.11}$$

Now choosing $dH_0/d\sigma_1 = 3.7 \times 10^{-4}$ gauss/atm to fit the experimental points at small t, we obtain $\delta_1 = 0.43$ and

$$\beta_1(T) = 3.7 \times 10^{-4} (f - 0.43f't) \text{ gauss/atm}.$$
 (5.12)

This value of δ_1 is comparable to the value of the same quantity found for Pb by Garfinkel and Mapother, ²⁴ their quantity $B \equiv (d \ln T_c/dp)/(d \ln H_0/dp) = 0.563$, rather than the value 1.0 predicted by double similarity, Eq. (3.30). The solid curve in Fig. 4 is (5.12), the points are measured values, ⁵ and the dashed curve is the one predicted by double similarity (and the value of β_1 at t = 1), given by (3.31), where $dH_0/d\sigma_1$ is evaluated from (5.11) with $\delta_1 = 1$, hence its equation is

$$\beta_1(T) = 1.58 \times 10^{-4} (f - f't) \text{ gauss/atm}.$$
 (5.13)

Thus (5.12) based on simple similarity satisfactorily reproduces the observed values, whereas (5.13) based

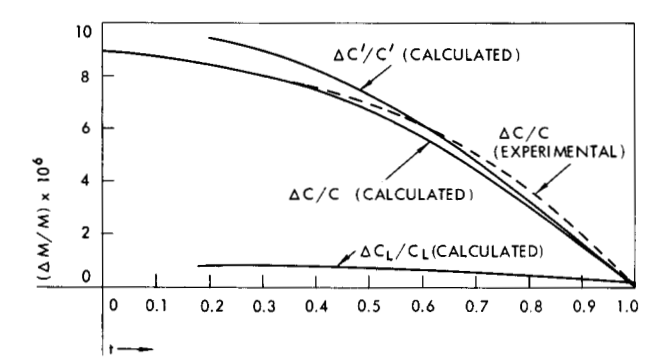


Figure 5 Calculated values of relative jump at the transition of the elastic moduli associated with particular elastic wave velocities, determined from critical field data, simple similarity, and β11, β12, β44 at Tc according to procedure in the text. Dashed curve is experimental values of Alers and Waldorf for ΔC/C.

on double similarity is in marked disagreement and shows the wrong trend with T. The calculated curve could be made to go through the cluster of points around $t^2=0.9$, but has been fixed by the value found above for β_1 at $t^2=1.0$, (5.2a). This value agrees, in fact, with the plotted measured point at $t^2=1.0$, which comes from the dT_c/dp of Jennings and Swenson, and is 2.7% lower than the value obtained from Hinrichs and Swenson, as noted just after (5.3). Thus simple similarity appears to hold for Ta very much the way it does for Pb.

Note that $\beta_1(T)$ and $H_c(T)$ fix the jump in strain at the transition, as given by (3.10). Since there are no data on Ta, we shall not give a curve. It is perhaps worth noting that the jump is negative, and the maximum magnitude, at 0° K, is

$$\Delta_{\rm tr} \varepsilon_1 = -2.4 \times 10^{-8} \,, \quad (0^{\circ} \rm K) \,.$$
 (5.14)

This may be compared with the magnetostrictive change given by (3.11), which is also negative and is proportional to the field squared; its maximum value at 0°K, is, using (A3.5b),

$$\Delta_{H_c} \varepsilon_1 = -0.45 \times 10^{-8} \,, \quad (0^{\circ} \text{K}) \,.$$
 (5.15)

Thus the magnetostrictive change is at most 20% of the jump.

Finally, we make a more tentative calculation based on similarity in predicting the temperature dependence of β_{11} , β_{12} , β_{44} or, equivalently of $\Delta_{tr}C/C$, $\Delta_{tr}C'/C'$, $\Delta_{tr}C_L/C_L$, from the values of β_{11} , β_{12} , β_{44} at T_c . This calculation will illustrate a type of analysis that should be very useful in fixing the second-order constants and checking the accuracy of the independent techniques used to obtain them, by relating critical field shift measurements to sound velocity jump measurements; also it will indicate the general trends with T—but we

do not have adequate data for reliable quantitative statements at this time.

The procedure followed, which involves a number of plausible assumptions of uncertain accuracy, will be sketched, but not given in detail. It is based on the equations (3.28) for $\beta_{ij}(T)$ from similarity, and (3.16) for the jumps in elastic moduli at the transition. From (3.28) we have

$$\beta_{11} = H_{0,11}(f - \delta_{11}f't) + (H_{0,1}^2/H_0)(2tf'_{1}(\delta_{1} - 1) + f''t^2), \quad (5.16a)$$

$$\beta_{12} = H_{0,12}(f - \delta_{12}f't) + (H_{0,1}^2/H_0)(2tf'\delta_1(\delta_1 - 1) + f''t^2), \quad (5.16b)$$

$$\beta_{44} = H_{0.44}(f - \delta_{44}f't). \tag{5.16c}$$

We first use (5.16c) to fit the values of β_{44} found from measured $\Delta_{tr}C/C$ values by (3.16a), and previously used to extrapolate the value of $\beta_{44}(T_c)$ in (5.6). A close fit is not possible since the peak in β_{44} is not reproduced when the ends of the curves are fitted; we therefore arbitrarily choose to fit at the ends (1.5°K and T_c), giving

$$H_{0.44} = 1.58 \times 10^{-7} \text{ gauss/atm}^2$$
, $\delta_{44} = 0.55$. (5.17)

The $\Delta C/C$ thereby fixed is shown in Fig. 5, with some of the experimental values of Alers and Waldorf. We then determine $H_{0,11}$ and $H_{0,12}$ to satisfy (5.16a) and (5.16b) at T_c , using the values in (5.7), assuming, in the absence of more data, that

$$\delta_{11} = \delta_{12} = \delta_{44} = 0.55, \tag{5.18}$$

and using the values of $H_{0,1}$ and δ_1 determined in the application of similarity to $\beta_1(T)$ (Footnote 25). This gives

$$H_{0,11} = 9.0 \times 10^{-8} \text{ gauss/atm}^2$$

$$H_{0.12} = -5.0 \times 10^{-8} \text{ gauss/atm}^2$$
, (5.19)

and fixes $\beta_{11}(T)$, $\beta_{12}(T)$ through (5.14a, b), hence determines $\Delta C'/C'$ and $\Delta C_L/C_L$ as functions of T through (3.16b, c) (Footnote 26). These curves are also plotted in Fig. 5.

Reliable data are not available, but the preliminary results do show $\Delta C_L/C_L$ small (in fact going negative at low t) compared to $\Delta C/C$, and $\Delta C'/C'$ larger than $\Delta C/C$, but apparently an order of magnitude larger and negative. Further study is needed; annealing treatment and impurity content may have drastic effects on the behaviors. Note that the relative longitudinal wave elastic modulus jump, $\Delta C_L/C_L$, is finite at t=1.0, whereas the shear wave moduli jumps vanish. This corresponds to the term $9B^2\beta_1^2/4\pi C_L$ in (3.16c) whose magnitude is 0.084×10^{-6} . The relative jump in Ta at T_c is small; for comparison, the same quantity in Pb is 2.5×10^{-6} , corresponding to elastic moduli four times smaller, but to a β_1 ten times larger, hence a factor overall of 25 larger.

5.4 Uniaxial stress data for tin

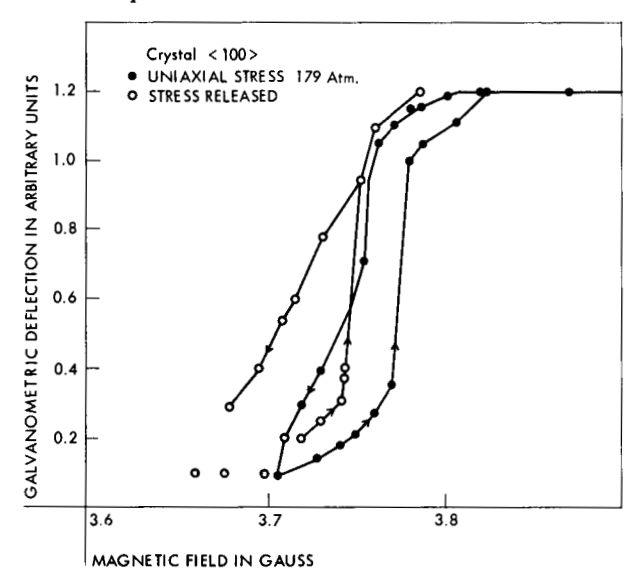
Due to the much lower strength of Sn compared to Ta, the uniaxial stress measurements are restricted to much lower levels. Thus the typical transition curves shown in Fig. 6 under 179 atm of uniaxial tension, correspond to a displacement of only hundredths of a gauss. The $\Delta_{\sigma}H_{c}$ curve derived from these transition curves is shown in Fig. 7 up to 200 atm. In fact, measurements of the strain show that plastic flow sets in at about 170 atm, in contrast to Ta, where the linear stress-strain region extends to more than 6000 atm of tension (provided the maximum load has been introduced and removed at least once). Another complication is the occurrence of hysteresis, indicated in Fig. 6, but the shift under stress can be extracted by comparing curves in increasing fields.

Successful measurements of shift were made only with specimens oriented along $\langle 100 \rangle$ (the diad or a-axis). Attempts to measure specimens with orientation close to $\langle 001 \rangle$ (the tetrad or c-axis) gave distorted transition curves under stress with no well-defined shift. This may be due to the generation of bending stresses, which will occur when the orientation is not exactly $\langle 001 \rangle$ and if the end of the specimen is clamped. This possibility is being studied further.

The data in Fig. 7 were fitted to a straight line through the origin by least squares.²⁸ Since the crystal axis was determined by X-rays to make an angle θ with the $\langle 001 \rangle$ axis of 87.5 \pm 0.5°, this gave, using (2.18b),

$$0.998\beta_1 + 0.002\beta_3 = (1.07 \pm 0.29) \times 10^{-4} \text{ gauss/atm}.$$
 (5.19)

Figure 6 Magnetic moment vs applied magnetic field for tin crystal, axis orientation (100). Points under uniaxial stress of 179 atm, •; points after release of stress, o; arrows indicate measurement with increasing and decreasing field, and show hysteresis. Temperature about 3.71°K.



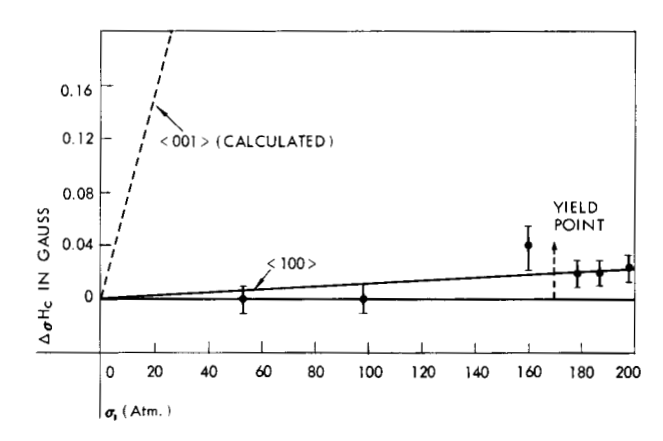


Figure 7 Critical field shift vs uniaxial stress for tin single crystal, axis orientation 2.5° from $\langle 100 \rangle$ (diad axis). The dashed line shows the calculated effect along the $\langle 001 \rangle$ (tetrad) axis, the full line is a least-squares straight-line fit to measured points going through the origin, slope $(1.07 \pm 0.29) \times 10^{-4}$ gauss/atm.

To evaluate β_1 and β_3 individually, we use the hydrostatic pressure coefficients which, by (2.17), give $(2\beta_1 + \beta_3)$. The most recent careful measurement by Jennings and Swenson⁴ gives $(dT_c/dp)_{T_c} = -(4.95 \pm 0.1)$ deg/atm, which combined with $(\partial H_c/\partial T)_{T_c} = -148.8$ gauss/deg,²⁹ leads to

$$-(\partial H_c/\partial p)_{T_c} = 2\beta_1 + \beta_3$$

= (7.37 \pm 0.15) \times 10^{-3} gauss/atm . (5.20)

However, the careful measurement of Fiske³ on the shift of H_c under p gives

$$-(\partial H_c/\partial p)_{T_c} = (6.56 \pm 0.15) \times 10^{-3} \text{ gauss/atm}.$$
 (5.21)

The reason for this discrepancy, which lies well outside the random error, has not been established, although Jennings and Swenson⁴ suggest that possibly polycrystalline and single crystal samples show different behavior. If this is the case, we shall be more interested in Fiske's value. Combining (5.19) first with (5.20), then with (5.21), gives

$$\beta_1 = (0.09 \pm 0.03) \times 10^{-3} \text{ gauss/atm},$$
(both cases), (5.22a)

$$\beta_3 = (7.18 \pm 0.15) \times 10^{-3} \text{ gauss/atm},$$
(polycrystalline result), (5.22b)

$$\beta_3 = (6.37 \pm 0.15) \times 10^{-3} \text{ gauss/atm},$$
(single crystal result). (5.22c)

These results may be compared with those of Grenier,² who made measurements on single-crystal

tin like the present ones, and obtained uniaxial stress coefficients for several values of θ . By extrapolating his measurements at each angle as a function of T to T_c , we obtain the values $(\partial H_c/\partial \sigma)_{T_c} \times 10^3$ gauss/atm = 6.32, 4.47, 2.44, 0.57 at $\theta = 13^\circ$, 33°, 53°, 87°, respectively. These are not quite linear in $\cos^2 \theta$, as (2.18b) would require, hence we choose only the two extreme values as the most reliable, (since the perturbing effects of bending stresses would be smallest) to define a straight line which extrapolates to

$$\beta_1 = 0.57 \times 10^{-3} \text{ gauss/atm},$$
 (5.23a)

$$\beta_3 = 6.61 \times 10^{-3} \text{ gauss/atm} \,.$$
 (5.23b)

Thus β_3 comes out much closer to the single-crystal value, (5.22c), and almost within the quoted error, which is consistent with the suggestion above that polycrystalline and single-crystal behavior differ. The β_1 value, however, comes out considerably larger than (5.22a). We note in support of our value that some of Grenier's other samples do show a good bit of scatter in β_1 values, 30 and also that a second sample of ours, which was not measured quantitatively, also showed considerably smaller β_1 than (5.23a). A further argument against (5.23a) is that (5.23a) and (5.23b) combined give $-(\partial H_c/\partial p)_{T_c} = (2\beta_1 + \beta_3) = 7.75 \times 10^{-3}$ gauss/atm, which is *not* in agreement with Fiske, (5.21), and even exceeds (5.20).

The settling of these differences awaits further data, which we hope may be partly provided by analysis of our tin measurements at intermediate values of θ , and by torsional measurements on single-crystal wires.

In any case, it is well established that tin shows a strong critical field-stress anisotropy, and from our values, stress along the c axis has over 70 times the effect of stress along the a axis. The very small a axis effect may in fact be regarded as an accidental cancellation of a hydrostatic effect and a shear effect of opposite sign, both produced by the uniaxial stress, as we see explicitly from (2.18b) with $l_3 = 0$. However, this great anisotropy is not present in the critical field-strain coefficients, which are more direct measures of the physical effect of deformation on superconductivity. Thus from the inverse of (A2.9a, b), with elastic constants at 4.2°K (Ref. 31), $C_{11} = 0.8166 \times 10^6$, $C_{12} = 0.570 \times 10^6$, $C_{13} = 0.3376 \times 10^6$, $C_{33} = 1.0175 \times 10^6$, $C_{44} = 0.2660 \times 10^6$, $C_{66} = 0.2781 \times 10^6$, all in atm; using (5.22a, c), we have

$$\alpha_1 = 2.28 \times 10^3 \text{ gauss}, \quad \alpha_3 = 6.54 \times 10^3 \text{ gauss},$$

$$\alpha_3/\alpha_1 = 2.87. \quad \text{(Footnote 32)}. \quad (5.24)$$

5.5 Remarks on similarity in tin

Grenier studied the T dependence of the coefficients β_1 and β_3 for tin, and Fiske, Muench and others studied the hydrostatic coefficient, $\beta_p(T)$. The results have been compared with the prediction of double similarity, which fixes the curve from the value at T_c , and most measured values come close to this predicted

curve. However, in view of the discussion in Section 3.5, this correspondence is probably accidental, and we wish to point out that Fiske's extensive careful measurements, although they show considerable scatter, seem to lie significantly above the double similarity curve. This is the direction of deviation from double similarity shown by a number of other superconductors, e.g., Ta, In, Pb. In view of the fact that these results were on single crystals, and in view of the verification of the value at T_c suggested in Section 5.4 on using our value of β_1 and Grenier's value of β_3 , we have compared Fiske's data in Fig. 8 with a curve based on simple similarity as well as the one from double similarity. The two parameters δ_p , and $H_{0,p}$ (Footnote 33) in (5.25) are chosen to fit at t = 1, and to follow the other points near T_c , which are believed more accurate than points at still lower T (giving more weight to the lower T points would raise the value of

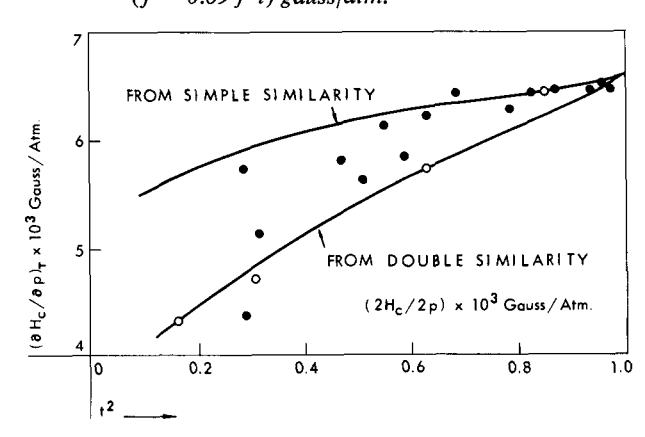
The equation, whose form is obtained from (3.23) on combining the equations for $H_{c,3}$ and $H_{c,1}$, is

$$\begin{split} \beta_p &\equiv (\partial H_c/\partial p)_T = H_{0,p}(f - \delta_p f't) \,, \\ H_{0,p} &= -(2H_{0,1} + H_{0,3}) = -5.28 \times 10^{-3} \text{ gauss/atm} \,, \\ \delta_p &= H_0 T_{c,p}/T_c H_{0,p} = 0.69 \,, \\ T_{c,p} &= -(2T_{c,1} + T_{c,3}) \,. \end{split} \tag{5.25}$$

Because of the great anisotropy in tin $\delta_p \cong \delta_3$. This value of δ_p may be compared with 0.43 for Ta in Eq. (5.12), 0.562 for Pb²¹ and 0.69 for In from Muench's data.³⁴ However, the situation is confused by the fact that Muench finds double similarity obeyed well for Sn. An additional puzzle is created by the

Figure 8 Critical field-pressure coefficient, $(\partial H_c | \partial p)_T$, vs t², for tin, measurements of Fiske, \circ ; measurements of Grenier, \bullet .

Lower curve calculated from double similarity and fitted to -6.56×10^{-3} gauss/atm, at t=1, $H_{c,p}=-3.65 \times 10^{-3}$ (f-f't); upper curve calculated from simple similarity fitted at t=1 and at lower t, $H_{c,p}=-5.28 \times 10^{-3}$ ($f-0.69 \ f't$) gauss/atm.



single crystal In data of Rohrer,³⁵ in which $H_{c,1}$ and $H_{c,3}$ are obtained from measured jumps in length at H_c (Eq. 3.10). Rohrer finds

$$\beta_3 = (3.4 + 2.8t^2) \times 10^{-3} \text{ gauss/atm},$$

 $\beta_1 = (0.20 + 0.10t^2) \times 10^{-3} \text{ gauss/atm}.$ (5.26)

Now from (3.23), on assuming the parabolic law, $f = 1 - t^2$, we obtain equations of the observed form, namely

$$\beta_i \cong H_{0,i}[1 + (2\delta_i - 1)t^2],$$
(parabolic approximation). (5.27)

Then (5.26) and (5.25) give³⁶

$$\delta_3 = 0.91 \; , \quad \delta_1 = 0.75 \; ,$$

$$\delta_{p} = -\frac{H_{0}}{T_{c}} \frac{1}{H_{c,T_{c}}} \frac{(2H_{c,1} + H_{c,3})_{T=T_{c}}}{(2H_{0,1} + H_{0,3})}$$

$$\approx \frac{1}{2} \frac{(2H_{c,1} + H_{c,3})_{T=T_{c}}}{(2H_{0,1} + H_{0,3})} = 0.89 ,$$
(5.28)

and this value of δ_p disagrees with the value deduced from Muench's data. More single-crystal work on In should resolve these questions.

5.6 Discussion

These two applications of the uniaxial stress technique, to Ta and Sn, illustrate two useful features of this technique in probing the behavior of superconductors under stress—the study of the second-order coefficients and of the anisotropy of the coefficients; also the first-order hydrostatic coefficients may be obtained fairly easily. Of course, more of the labor of carrying out the experiment is shifted to the preparation of suitable single-crystal specimens.

Confidence in the accuracy of the measurements is established by the satisfactory agreement on the value of $(\partial H_c/\partial p)_{T_c}$ obtained here, with the value from other recent work on specially purified Ta. The second-order contribution seems clearly established, and its general magnitude is confirmed by the recent measurements of sound velocity jumps at the transition. The actual values of the second-order coefficients are still tentative owing to the uncertainty in the sound velocity measurements, which are not on good specimens, and to the fact that no specimens of Ta for uniaxial stress have been successfully prepared with different orientation than $\langle 110 \rangle$. It is worth noting that the secondorder coefficients are nonlinear effects in the superconducting properties, and not in the elastic properties, since all measurements are well within the Hooke's law region. The second-order contribution to $\Delta_{\sigma}H_{c}$ is already 10% at 1000 atm (along $\langle 110 \rangle$), and is 40% at 6000 atm. Since no second-order effects are detected out to 10,000 atm of hydrostatic pressure, it follows that the second-order effects are much more sensitive in Ta to shear stresses, although by virtue of the cubic symmetry the first-order shear effects vanish.

Similarity is a valuable tool in predicting and testing the observed temperature dependences, although it has not been derived from first principles; however it is necessary to work with the less restrictive form, called simple similarity, which allows H_0 and T_c to vary independently with stress, hence has two parameters to fix. Then Ta appears to obey simple similarity, as shown from the behavior of $(\partial H_c/\partial p)_T$ with T, but with a rather small value of the dimensionless parameter $\delta_1 = (\partial \ln T_c/\partial p)/(\partial \ln H_0/\partial p)$. The value $\delta_1 = 0.43$ is the smallest of those for the four superconductors Ta, Pb, In, Sn, and gives $(\partial H_c/\partial p)_T$ for Ta a trend with T opposite to that of the other three.

Furthermore, tentative application of similarity makes possible prediction of the behavior of the sound velocity elastic-modulus jumps as a function of T, so that detailed cross-checks between these two completely independent experiments on the second-order constants should be possible, and very useful in spotting systematic error in either.

The remarkable anisotropy of the first-order coefficients of tin to uniaxial stress found by Grenier is confirmed, and our new value for the smaller coefficient, β_1 , which is a factor six smaller than Grenier's, makes this anisotropy still greater. Combining this value of β_1 with Fiske's single-crystal hydrostatic measurement gives a value of β_3 that checks well with Grenier's, whereas using the polycrystalline hydrostatic measurement of Jennings and Swenson leads to a substantially greater value than Grenier's. This seems a further indication of a difference between single-crystal and polycrystalline measurements, suggested by Jennings and Swenson in consequence of the discrepancy between the two hydrostatic coefficients.

If new weight is put on Fiske's single-crystal measurements, then his values of $(\partial H_c | \partial p)_T$ at various T indicate some deviation from the behavior predicted from the more restrictive form of similarity (double similarity) which previously seemed confirmed by polycrystalline measurements on tin. A tentative value of the constant δ_p is suggested from these data. In addition the value of δ_p for In is still uncertain, since new single-crystal data, which are derived, however, from the difficult technique of measuring length jumps at the transition, disagree with older data on polycrystalline In.

A general conclusion is that more single-crystal data are both desirable and necessary to settle some of these problems in Ta, Sn, and In. In addition much remains to be explored about the anisotropy of the various coefficients.³⁷ Higher precision data would be needed to test the validity of simple similarity since, to present accuracy, it seems to hold for all measurements.

Appendix I: Strain and stress notation and relations

The second-rank stress tensor with components σ_{ij} , i, j = 1, 2, 3 denotes the force per unit area in the

j direction on the face perpendicular to the i axis. Since it is a symmetrical tensor, there are six independent components. Thus the tensor is commonly and conveniently given in single index notation by

$$\begin{bmatrix} \sigma_1 & \sigma_6 & \sigma_5 \\ \sigma_6 & \sigma_2 & \sigma_4 \\ \sigma_5 & \sigma_4 & \sigma_3 \end{bmatrix} \equiv \begin{bmatrix} \sigma_{11} & \sigma_{12} & \sigma_{13} \\ \sigma_{12} & \sigma_{22} & \sigma_{23} \\ \sigma_{13} & \sigma_{23} & \sigma_{33} \end{bmatrix}. \tag{A1.1}$$

Similarly, the symmetrical second-rank infinitesimal strain tensor with components ε_{ij} , i, j = 1, 2, 3, denotes the gradient in the i (or j) direction of the symmetrized displacement in the j (or i) direction. In single index notation it has the form

$$\begin{bmatrix} \varepsilon_1 & \varepsilon_6/2 & \varepsilon_5/2 \\ \varepsilon_6/2 & \varepsilon_2 & \varepsilon_4/2 \\ \varepsilon_5/2 & \varepsilon_4/2 & \varepsilon_3 \end{bmatrix} \equiv \begin{bmatrix} \varepsilon_{11} & \varepsilon_{12} & \varepsilon_{13} \\ \varepsilon_{12} & \varepsilon_{22} & \varepsilon_{23} \\ \varepsilon_{13} & \varepsilon_{23} & \varepsilon_{33} \end{bmatrix}$$

or
$$\begin{cases} \varepsilon_{i} = m_{i}\varepsilon_{i1i2}, \\ m_{i} = 1, & i = 1, 2, 3, \\ m_{i} = 2, & i = 4, 5, 6. \end{cases}$$
 (A1.2)

where i_1i_2 is the two-index form corresponding to i.

For small strains we assume linear phenomenological relations between stress and strain in the form

$$\varepsilon_{ij} = \sum_{k,l=1}^{3} S_{ijkl} \sigma_{kl} , \quad \sigma_{kl} = \sum_{i,j=1}^{3} C_{klij} \varepsilon_{ij} , \qquad (A1.3)$$

where the S_{ijkl} are the elastic compliance coefficients, and the C_{ijkl} the elastic moduli. These are each fourthrank symmetrical tensors, and are usually written in a reduced two-index form defined by

$$\varepsilon_i = \sum_{j=1}^6 S_{ij} \sigma_j , \qquad (A1.4a)$$

$$\sigma_j = \sum_{i=1}^6 C_{ji} \varepsilon_i \,, \tag{A1.4b}$$

where

$$S_{ij} \equiv m_i m_j S_{i1i2j1j2} ,$$
 (A1.5a)

$$C_{ji} \equiv C_{j1j2i1i2}$$
 (A1.5b)

Of interest for the applications in this work are three special stresses:

(1) hydrostatic stress of magnitude σ , a normal stress of equal magnitude on all surfaces, whose components in single index form, written as a row vector of six components, are

(2) uniaxial stress of magnitude σ , in the direction with direction cosines l_1 , l_2 , l_3 , given by

$$\sigma_{\text{uniax}} \equiv (l_1^2 \sigma, l_2^2 \sigma, l_3^2 \sigma, l_2 l_3 \sigma, l_3 l_1 \sigma, l_1 l_2 \sigma). \quad (A1.7)$$

(3) shear stress of magnitude σ , either in the direction l_1 , l_2 , l_3 on a surface tangential to l_1 , l_2 , l_3 and normal to m_1 , m_2 , m_3 , or with l_1 , l_2 , l_3 and m_1 , m_2 , m_3 interchanged; the components are given by

$$\sigma_{\text{shear}} \equiv (2l_1 m_1 \sigma, 2l_2 m_2 \sigma, 2l_3 m_3 \sigma, (l_2 m_3 + l_3 m_2) \sigma,$$

$$(l_3m_1 + l_1m_3)\sigma, (l_1m_2 + l_2m_1)\sigma), \quad (A1.8)$$

where
$$l_1 m_1 + l_2 m_2 + l_3 m_3 = 0$$
. (A1.9)

For cubic symmetry, there are three independent elastic constants, the tensors having the form given in (2.9). The C_{ij} and S_{ij} tensors are reciprocals, from which follows easily

$$(C_{11} - C_{12})(S_{11} - S_{12}) = 1$$
, (A1.10a)

$$(C_{11} + 2C_{12})(S_{11} + 2S_{12}) = 1$$
, (A1.10b)

$$C_{44}S_{44} = 1. (A1.10c)$$

Three elastic moduli defined by elastic wave velocities, v, are also of interest here, namely

$$C_L = \rho v_L^2 = (C_{11} + C_{12} + 2C_{44})/2$$
 (A1.11a)

for a longitudinal wave in (110) direction,

$$C = \rho v_{t_1}^2 = C_{44} \tag{A1.11b}$$

for a transverse wave in $\langle 110 \rangle$ direction, polarized parallel to the $\langle 001 \rangle$ axis,

$$C' = \rho v_{t_2}^2 = (C_{11} - C_{12})/2$$
 (A1.11c)

for a transverse wave in the $\langle 110 \rangle$ direction, polarized parallel to $\langle \overline{1}10 \rangle$.

The bulk modulus of a cubic crystal is

$$B = -V \frac{dp}{dV} = \frac{C_{11} + 2C_{12}}{3} = \frac{1}{3(S_{11} + 2S_{12})}. \text{ (A1.12)}$$

The Young's modulus Y in the direction l_1 , l_2 , l_3 , defined as the ratio of a uniaxial stress in the l_1 , l_2 , l_3 direction to the corresponding longitudinal strain is given by

$$\frac{1}{Y} = S_{11} + 2[S_{44}/2 - (S_{11} - S_{12})] \times (l_2^2 l_3^2 + l_3^2 l_1^2 + l_1^2 l_2^2). \tag{A1.13}$$

Appendix 2: Relations between critical fieldstress and critical field-strain coefficients

From (2.2), (2.5) and (A1.4a) we have

$$\beta_i = \frac{\partial H_c(T, \sigma_i)}{\partial \sigma_i} = \sum_{j=1}^6 \frac{\partial H_c}{\partial \varepsilon_i} \frac{\partial \varepsilon_j}{\partial \sigma_i} = \sum_{j=1}^6 \alpha_j S_{ji}. \quad (A2.1)$$

Similarly, from (2.3), (2.6) and (A1.4a) we have

$$\beta_{ij} = \sum_{k=1}^{6} S_{ki} S_{lj} \alpha_{kl} , \qquad (A2.2)$$

and inversely, using (A1.4b), we have

$$\alpha_i = \sum_{j=1}^6 \beta_j C_{ji} \tag{A2.3}$$

$$\alpha_{ij} = \sum_{k=1}^{6} C_{ki} C_{lj} \beta_{kl} . \tag{A2.4}$$

For cubic symmetry, using the simplified forms of the tensors in (2.9), we obtain

$$\beta_1 = (S_{11} + 2S_{12})\alpha_1 \,, \tag{A2.5}$$

$$\beta_{11} = (S_{11}^2 + 2S_{12}^2)\alpha_{11} + 2S_{12}(2S_{11} + S_{12})\alpha_{12} ,$$
 (A2.6a)

$$\beta_{12} = S_{12}(2S_{11} + S_{12})\alpha_{11} +$$

$$+ (S_{11}^2 + 2S_{11}S_{12} + 3S_{12}^2)\alpha_{12} , \qquad (A2.6b)$$

$$\beta_{44} = S_{44}^2 \alpha_{44} \,, \tag{A2.6c}$$

and inversely

$$\alpha_1 = (C_{11} + 2C_{12})\beta_1 , \qquad (A2.7)$$

$$\alpha_{11} = (C_{11}^2 + 2C_{12}^2)\beta_{11} + 2C_{12}(2C_{11} + C_{12})\beta_{12} \; , \eqno(A2.8a)$$

$$\alpha_{12} = C_{12}(2C_{11} + C_{12})\beta_{11} + (C_{11}^2 + 2C_{11}C_{12} + 3C_{12}^2)\beta_{12}, \qquad (A2.8b)$$

$$\alpha_{44} = C_{44}^2 \beta_{44} \,. \tag{A2.8c}$$

For tetragonal symmetry, using the appropriate tensors given in (2.15),

$$\beta_1 = (S_{11} + S_{12})\alpha_1 + S_{13}\alpha_3, \qquad (A2.9a)$$

$$\beta_3 = 2S_{13}\alpha_1 + S_{33}\alpha_3 \,, \tag{A2.9b}$$

$$\begin{split} \beta_{11} &= (S_{11}^2 + S_{12}^2)\alpha_{11} + 2S_{11}S_{12}\alpha_{12} \\ &+ 2S_{13}(S_{11} + S_{12})\alpha_{13} + S_{13}^2\alpha_{33} \;, \end{split} \tag{A2.10a}$$

$$\begin{split} \beta_{12} &= 2S_{11}S_{12}\alpha_{11} + (S_{11}^2 + S_{12}^2)\alpha_{12} \\ &+ 2S_{13}(S_{11} + S_{12})\alpha_{13} + S_{13}^2\alpha_{33} \;, \end{split} \tag{A2.10b}$$

$$\begin{split} \beta_{13} &= S_{13}(S_{11} + S_{12})(\alpha_{11} + \alpha_{12}) \\ &+ (S_{11}S_{33} + S_{12}S_{33} + 2S_{13}^2)\alpha_{13} + S_{13}S_{33}\alpha_{33} \;, \end{split}$$
 (A2.10c)

$$\beta_{33} = 2S_{13}^2(\alpha_{11} + \alpha_{12}) + 4S_{13}S_{33}\alpha_{13} + S_{33}^2\alpha_{33},$$
(A2.10d)

$$\beta_{44} = S_{44}^2 \alpha_{44} \,, \tag{A2.10e}$$

$$\beta_{66} = S_{66}^2 \alpha_{66} . \tag{A2.10f}$$

The corresponding formulas for α in terms of β are obtained from (A2.9) and (A2.10) by interchange of α and β and replacement of S_{ij} 's by C_{ij} 's.

Appendix 3: Summary of critical field and other data for tantalum

It is convenient to work with the values of the deviation function, $^{38}\delta h$, against t^2 , where

$$\delta h \equiv f - (1 - t^2)$$
, $f(t) \equiv H_c/H_0$, $t \equiv T/T_c$. (A3.1)

Then we have

$$f = 1 - t^2 + \delta h \,, \tag{A3.2a}$$

$$f' = -2t(1 - d\delta h/d(t^2)),$$
 (A3.2b)

$$f'' = 2d\delta h/d(t^2) + 4t^2d^2\delta h/d(t^2)^2 - 2.$$
 (A3.2c)

The data of Hinrichs and Swenson⁵ may be compactly summarized by the tabulation (from the smoothed curve in their Fig. 4).

Quadratic interpolations in this table will reproduce their curve to within a unit in the last significant figure and reproduce the experimental points to ± 0.5 gauss. (The values of $-\delta h$ from Shaw, Mapother and Hopkins, ³⁸ are quite close for $t^2 > 0.5$ but appear to be a few units larger in the last figure for $t^2 < 0.5$).

Applying (A3.2b), and second difference formulas, to (A3.3), we estimate

$$\left(\frac{\partial H_c}{\partial T}\right)_{T_c} = -337 \text{ gauss/deg},^{39} \quad f'(1) = -1.83_4,$$
(A3.4a)

$$\left(\frac{\partial^2 H_c}{\partial T^2}\right)_{T_c} = -72 \text{ gauss/deg}^2, \quad f''(1) = -1.75_6.$$
(A3.4b)

Elastic constants for Ta at 4.2°K,40

Elastic moduli (atm)

$$C_{11} = 2.681 \times 10^6$$

$$C_{12} = 1.600 \times 10^6$$

 $C_{44} = 0.865 \times 10^6$ (A3.5a)

$$C = 0.541 \times 10^6$$

$$C_L = 3.005 \times 10^6$$

$$B = 1.960 \times 10^6$$
.

Compliance coefficients (atm⁻¹)

$$S_{11} = 0.674 \times 10^{-6}$$

 $S_{12} = -0.252 \times 10^{-6}$ (A3.5b)
 $S_{44} = 1.156 \times 10^{-6}$
 $K = 0.510 \times 10^{-6}$

Acknowledgments

We should like to thank A. Burgess and P. Roland for assistance with the measurements, and D. J. Quinn and Y. Budo for assistance in the design and construction of the apparatus, all of the Thomas J. Watson Research Laboratory. We are indebted to G. Alers, Ford Scientific Laboratory, C. Swenson, Iowa State University, C. Grenier, Louisiana State University, and G. Cody of RCA Laboratories, for communication of various results, and to J. Swihart, of the Thomas J. Watson Research Laboratory, for discussion, particularly of the relation of BCS theory to similarity.

References and footnotes

- 1. A preliminary account has been published; D. P. Seraphim and Paul M. Marcus, *Phys. Rev. Letters* 6, 680 (1961).
- C. Grenier, Compt. Rend. 238, 2300 (1954); 240, 2302 (1955);
 241, 1275 (1955); Thesis, University of Paris, 1956 (unpublished).
- 3. M. D. Fiske, J. Phys. Chem. Solids 2, 191 (1957).
- L. D. Jennings and C. A. Swenson, *Phys. Rev.* 112, 31 (1958).
- C. H. Hinrichs and C. A. Swenson, *Phys. Rev.* 123, 1106 (1961).
- 6. Some basic definitions and formulas of crystal elasticity theory used here are given in Appendix I.
- 7. See, for example, C. S. Smith, "Symmetry and Properties of Crystals", in *Solid State Physics* 6, 215 and 237 (1958). (Edited by Seitz and Turnbull, Academic Press).
- 8. See C. S. Smith, *loc. cit.*, p. 237, four of the seven tetragonal point groups have the form in (2.15) for β_{ij} .
- 9. See, for example, D. Shoenberg, *Superconductivity*, Cambridge University Press, 1957, p.73.
- 10. An entirely analogous and complementary thermodynamic development to (3.2)–(3.12) may be based on a Helmholtz free energy (with respect to the mechanical variables), $F = E TS H_e M$, and changes at constant strain. Then at the transition $F_n(T, \varepsilon_i) = F_s(T, \varepsilon, H_c)$, and there are magnetostrictive and transition changes in stress at constant strain. Thus the latter has the form $\Delta_{\rm tr} \sigma_i = (H_c/4\pi)(\partial H_c/\partial \varepsilon_i)$ analogous to (3.10) and differentiation by ε_i gives

 $\begin{array}{l} \Delta_{\rm tr} C_{ij} = (\frac{1}{4}\pi)[(\partial H_c/\partial \varepsilon_i)(\partial H_c/\partial \varepsilon_j) + H_c(\partial^2 H_c/\partial \varepsilon_i\partial \varepsilon_j)] \\ = (\alpha_i\alpha_j + H_c\alpha_{ij}), \end{array}$

analogous to (3.12) (given also by Grenier² in his thesis). Since the condition of constant strain is not easily realized experimentally, the equation for $\Delta_{\rm tr}\sigma_i$ is not very interesting. However, the equation between $\Delta_{\rm tr}C_{ij}$ and the α 's is a definite relation between constants of the two phases, independent of stress; it must in fact be an algebraic consequence of (3.12) and the equations relating the C's and α 's with the S's and β 's.

- 11. J. Kok, *Physica* 1, 1103 (1934). The normal-state heat capacity is γT .
- 12. Equation (3.23) is given by Garfinkel and Mapother²⁴ in their Eq. (13); they refer to simple similarity as "geometric similarity," and use the symbol B for our δ .
- J. Bardeen, L. Cooper and R. Schrieffer, *Phys. Rev.* 108, 1175 (1957).

- 14. Of course, the values of $\partial F/\partial (kT_c/\hbar\omega)$ near $T/T_c=0$ or 1 are smaller, and approach zero, since F is fixed at those points. The maximum value of $\partial F/\partial (kT_c/\hbar\omega)$ approaches zero in the weak-coupling limit, $kT_c/\hbar\omega=0$, while the largest value that occurs is about 0.04 for Pb with $kT_c/\hbar\omega=0.075$. Detailed calculations of $H_c(T)/H_0$ and other reduced quantities have been made for all values of coupling strength, and will be reported separately. Included is the reduced energy gap, $\varepsilon_0(T)/\varepsilon_0(0)$, which also may be given in the form $F(T/T_c, \alpha)$ where α may be any of the parameters measuring the coupling; e.g., $(kT_c/\hbar\omega)$, $\varepsilon_0(0)/kT_c$, or $\varepsilon_0(0)/\hbar\omega$.
- 15. The values of $\partial T_c/\partial p$ are -0.26×10^{-5} deg/atm at $T_c = 4.5^\circ \text{K}$ for Ta, and -5×10^{-5} deg/atm at $T_c = 3.7^\circ \text{K}$ for Sn. The value of $\partial \ln \Theta/\partial p$ we deduce roughly from the Gruneisen constant $\gamma_G = -\partial \ln \Theta/\partial \ln V \cong 2$ for Ta and Sn. Since the compressibilities, $K = -\partial \ln V/\partial p \cong 0.5 \times 10^{-6}$ atm⁻¹ for both Ta and Sn, $\partial \ln \Theta/\partial p = \gamma_G K \cong 10^{-6}$ atm⁻¹ for both.
- D. P. Seraphim, J. I. Budnick, W. B. Ittner III, AIME Trans. 218, 527 (1960).
- 17. H. S. Sommers, Jr., Rev. Sci. Instr. 25, 793 (1954).
- 18. M. W. Garret, J. Appl. Phys. 22, 1091 (1951).
- No success was obtained in growing crystals of significantly different orientation.
- See, for example, the tabulation of values in J. L. Olsen and H. Rohrer, Helv. Phys. Acta 33, 872 (1960).
- 21. G. A. Alers and D. L. Waldorf, *Phys. Rev. Letters* 6, 677 (1961), and private communication on Ta.
- 22. Specializing (3.38) to cubic symmetry, and solving for β_{11} , gives

$$\begin{split} \left(\frac{\partial^2 H_c}{\partial p^2}\right)_{T_c} &= 9\beta_{11} = 9 \bigg[-\frac{1}{9} \frac{d^2 T_c}{dp^2} \frac{\partial H_c}{\partial T} + 2\beta_1 \frac{d\beta_1}{dT} \bigg/ \frac{\partial H_c}{\partial T} \\ &- \beta_1^2 \frac{\partial^2 H_c}{\partial T^2} \bigg/ \left(\frac{\partial H_c}{\partial T}\right)^2 \bigg]_{T=T_c} \,. \end{split}$$

Using (5.2a), (A3.4a), (A3.4b), and $(d\beta_1/dT)_{T_c}=-0.22\times 10^{-4}$ gauss/deg atm from measured values (see Fig. 4), gives (5.5).

- 23. Alers and Waldorf²¹ have measured the three velocity jumps yielding $\Delta C/C$, $\Delta C'/C'$, and $\Delta C_L/C_L$ (defined in (A.11)), as functions of T; however, only $\Delta C/C$ had a reasonable form and did not change substantially on annealing, hence we have based a discussion on it alone. We are indebted to Dr. Alers for communication of his preliminary results.
- M. Garfinkel and D. E. Mapother, *Phys. Rev.* 122, 459 (1961).
- 25. These should be $H_{0,1}=3.7\times10^{-4}$ gauss/atm, $\delta_1=0.43$, but in fact the values used in the calculation were slightly different, since they were based on an earlier analysis of β_1 , namely $H_{0,1}=3.3\times10^{-4}$ gauss/atm, $\delta_1=0.50$. This should not make any substantial difference in the curves of Fig. 5, which are, in any case, not of quantitative significance.
- 26. Note that (3.16a, b, c) are not consistent if C is in atm and $H_{0,ij}$ in gauss/atm², and unit conversion factors are needed
- 27. However, the shift shown in Fig. 6 is even smaller than implied by the factor 20 reduction in applied stress compared to the Ta transition curves in Fig. 4. At the orientation used, <100>, the uniaxial stress coefficient has its smallest value, and is in fact only one-third that of Ta, whereas for the orientation <001> the coefficient is over 20 times larger than for Ta, and the shifts would then be comparable (compare (5.22) and (5.20)).
- 28. An estimate of the second-order contribution in tin for tension along $\langle 100 \rangle$ indicates it could be appreciable, which would tend to reduce the magnitude of β_1 ; this is suggested also by the absence of observable shift at the lower pressures

53 and 98 atm. The estimate was made from the measured value $T_{c,pp} \equiv (\partial^2 T_c/\partial p^2) = 7.8 \times 10^{-10}$ deg/atm², leading to $\beta_{pp} = \partial^2 H_c/\partial p^2 \sim 10^{-7}$ gauss/atm². Hence if $\beta_{11} \equiv \partial^2 H_c/\partial \sigma_1^2$ is assumed to have the same magnitude, then the ratio of second- to first-order term for stress along $\langle 100 \rangle$ is $\beta_{11}\sigma_1^2/2\beta_1\sigma_1 \sim 10^{-1}$ at 200 atm. The relation used was (3.38) applied to pressure as the stress variable, and solved for β_{pp} in the form, using (3.37), $\beta_{pp} = -2T_{c,p}\beta'_p - T_{c,p}^2H''_c - T_{c,pp}H'_c$ where the primes are temperature derivatives at $T = T_c$. Then put $T_{c,p} = -4.95 \times 10^{-5}$ deg/atm, $\beta'_p \sim 10^{-3}$ gauss/atm deg (measured value, see Fig. 8), and from the critical field curve $H'_c = -148.8$ gauss/deg, $H''_c \cong -31$ gauss/deg².

- From J. F. Cochran and D. E. Mapother, *Phys. Rev.* 121, 1688 (1961), Table II.
- 30. C. Grenier, Comptes Rendus 240, 2302 (1955), Fig. 2.
- J. A. Rayne and B. S. Chandrasekhar, Phys. Rev. 120, 1658 (1960).
- 32. Fiske³ finds $\alpha_3/\alpha_1 = 2.6$; note his Eq. (8) for this ratio has a factor 2 missing, and should read

$$\frac{k_3}{k_1} = \frac{S_{11} + S_{12} - 2\alpha S_{13}}{\alpha S_{33} - S_{13}} \cdot$$

- 33. The comma notation for derivatives is defined in (3.22) to (3.29).
- 34. N. L. Muench, Phys. Rev. 99, 1814 (1955).
- 35. H. Rohrer, Phil. Mag. 4, 1207 (1959).
- 36. The parabolic law implies $H_{c,T_c} = -2H_0/T_c$.

- 37. For example: does simple similarity apply to each component coefficient separately, and if so, does each show the same value of δ; how well does similarity describe the second-order coefficients; how great is the anisotropy of the second-order effects, et cetera?
- Called D(t) by Shaw, Mapother, and Hopkins, Phys. Rev. 120, 88 (1960).
- 39. The value of $(\partial H_c/\partial T)_{T_c}$ in (A3.4a) has slightly greater magnitude than estimated by some previous workers; e.g., Cochran and Mapother, 29 give -327 gauss/deg. The difference could come from a slight bending down of the δh vs t^2 curve near $t^2 = 1$, i.e., a negative curvature, which is visible in Fig. 4 of Hinrichs and Swenson;5 it appears also on replotting the data of Shaw, Mapother and Hopkins,³⁸ although it is not detectable on the small-scale smooth curve of their Fig. 3. Further support for the value above comes from the critical field measurements of Seraphim, Novick and Budnick, Acta. Met., 9, 446 (1961) very near T_c on pure Ta, which give -336 gauss/deg, and from the calorimetric measurements of Chou, White, and Johnston, (who obtain $(\partial H_c/\partial T)_{T_c}$ from the jump in specific heat at T_c), Phys. Rev., 109, 797 (1958); these are probably not as sensitive to impurity content as magnetic measurements and give -334 gauss/deg.
- 40. G. A. Alers, private communication.

Received October 16, 1961